Non-Symmetric Benzene-Pyridine-Based Nickel Pincer Complexes featuring Borohydride, Formate, Ethyl and Nitrosyl Ligands

Daniel Himmelbauer,[†] Heiko Schratzberger,[†] Matthias G. Käfer,[†] Berthold Stöger,[‡] Luis F. Veiros,[¶] and Karl Kirchner[*,†]

†*Institute of Applied Synthetic Chemistry, Vienna University of Technology, Getreidemarkt 9, A-1060 Vienna, Austria*

‡*X-Ray Center, Vienna University of Technology, Getreidemarkt 9, A-1060 Vienna, Austria*

¶*Centro de Química Estrutural, Instituto Superior Técnico, Universidade de Lisboa, Av. Rovisco Pais No. 1, 1049-001 Lisboa, Portugal*

E-mail: karl.kirchner@tuwien.ac.at

Phone: (+43) 1 58801 163611. Fax: (+43) 1 58801 16399

Supporting Information

Ligand Syntheses

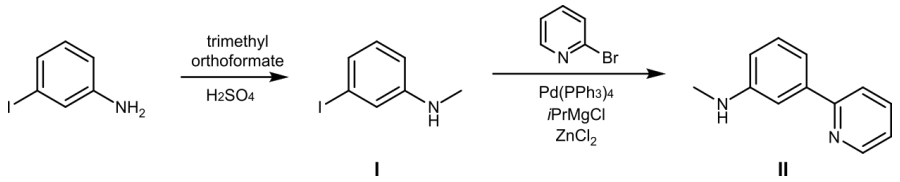

3-iodo-N-methylaniline (**I**) was prepared according to the literature.[1]

N-methyl-3-(pyridin-2-yl)aniline (**II**) was synthesized in a similar fashion to the literature.[2] To a solution of *i*PrMgCl (10.8 ml, 2.0 M in THF, 21.6 mmol) in a 50 ml three-neck round-bottom flask, 2-brompyridine (2.96 g, 18.7 mmol) was added slowly in a dropwise fashion while maintaining the reaction temperature below 20 °C with a water bath. After complete addition the reaction solution was stirred for 3 h at room temperature and then $ZnCl_2$ (3.14 g, 23.1 mmol) dissolved in THF (25 ml) was added slowly in a drop wise fashion while cooling again with a water bath to keep the temperature below 20 °C. The reaction mixture was stirred for another hour at room temperature and then transferred via syringe to another 100 ml three-neck round-bottom-flask containing **I** (3.16 g, 13.6 mmol) and $Pd(PPh_3)_4$ (211 mg, 1.3 mol%). The mixture was stirred at reflux for 24 h and then quenched with saturated NH_4Cl solution, extracted with EtOAc (3 x 40 ml) and washed with a saturated $Na_2S_2O_3$. The combined organic layers were dried over Na_2SO_4 and all volatiles were removed under reduced pressure yielding 2.96 g of the crude product as brown/orange oil which was purified by silica gel chromatography (ethyl acetate/ petrol ether 1:9) yielding 2.06 g (59 %) of the product in anatlytical pure form as brown oil. ^{1}H NMR (δ, 600 MHz, CD_2Cl_2, 20 °C): 8.73 (m, 1H, CH), 7.76 (m, 2H, CH), 7.40 (m, 2H, CH), 7.35 (m, 1H, CH), 7.24 (m, 1H, CH), 6.71 (m, 1H, CH), 4.16 (s, 1H, NH), 2.87 (s, 3H, NCH_3). $^{13}C\{^1H\}$ NMR (δ, 151 MHz, CD_2Cl_2, 20 °C): 157.9 (C), 150.4 (C), 149.7 (CH), 140.5 (C), 136.9 (CH), 129.7 (CH), 122.4(CH), 120.8 (CH), 115.8 (CH), 113.3 (CH), 110.9 (CH), 30.8 (NCH_3). HR-MS (ESI$^+$, CH_3CN/MeOH + 1 % H_2O): m/z calcd for $C_{12}H_{13}N_2$ $[M+H]^+$ 185.1079, found 185.1072.

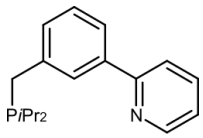

1b

2-(3-((diisopropylphosphaneyl)methyl)phenyl)pyridine (**1b**) was prepared according to the literature.[3]

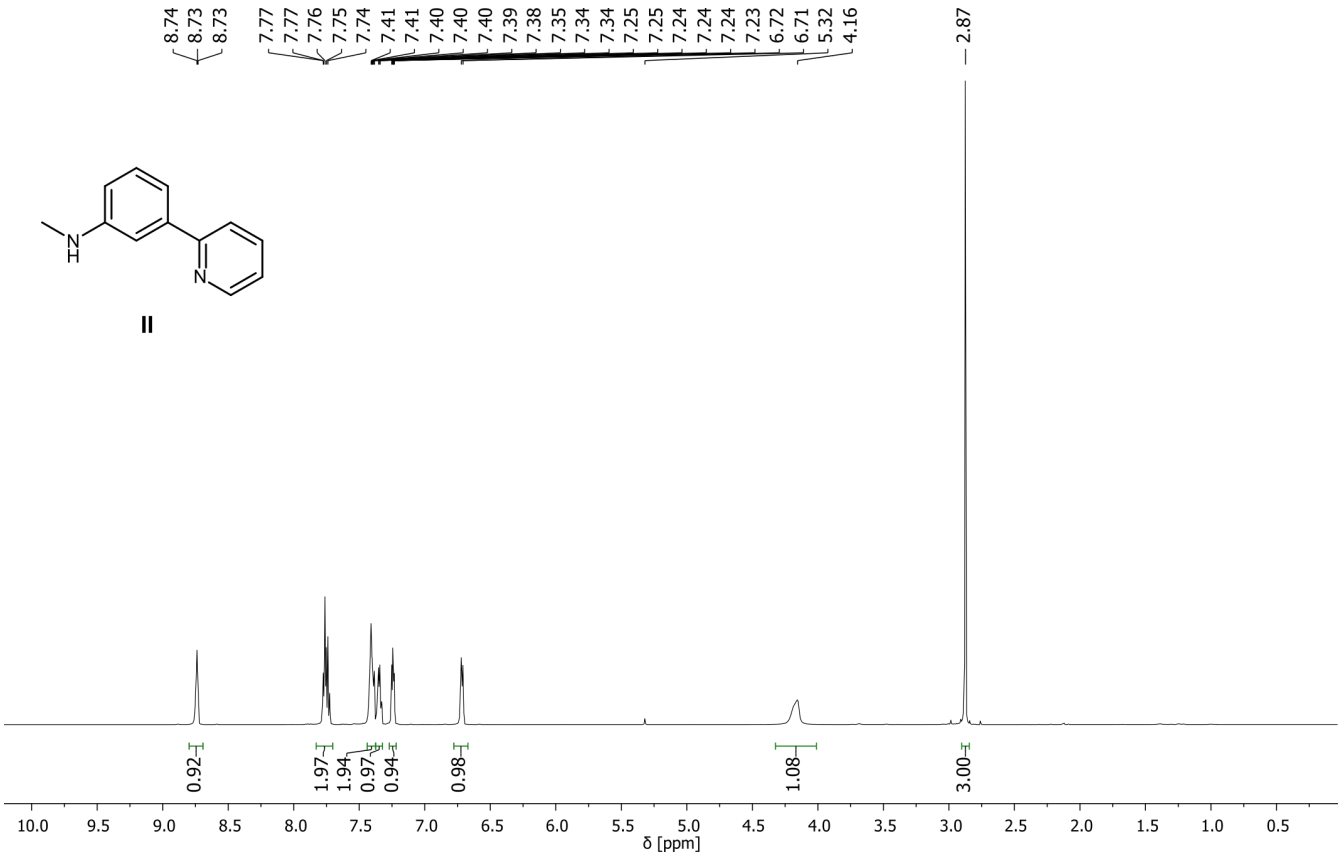

Figure S1. ^{1}H (600 MHz, CD_2Cl_2) *N*-methyl-3-(pyridin-2-yl)aniline

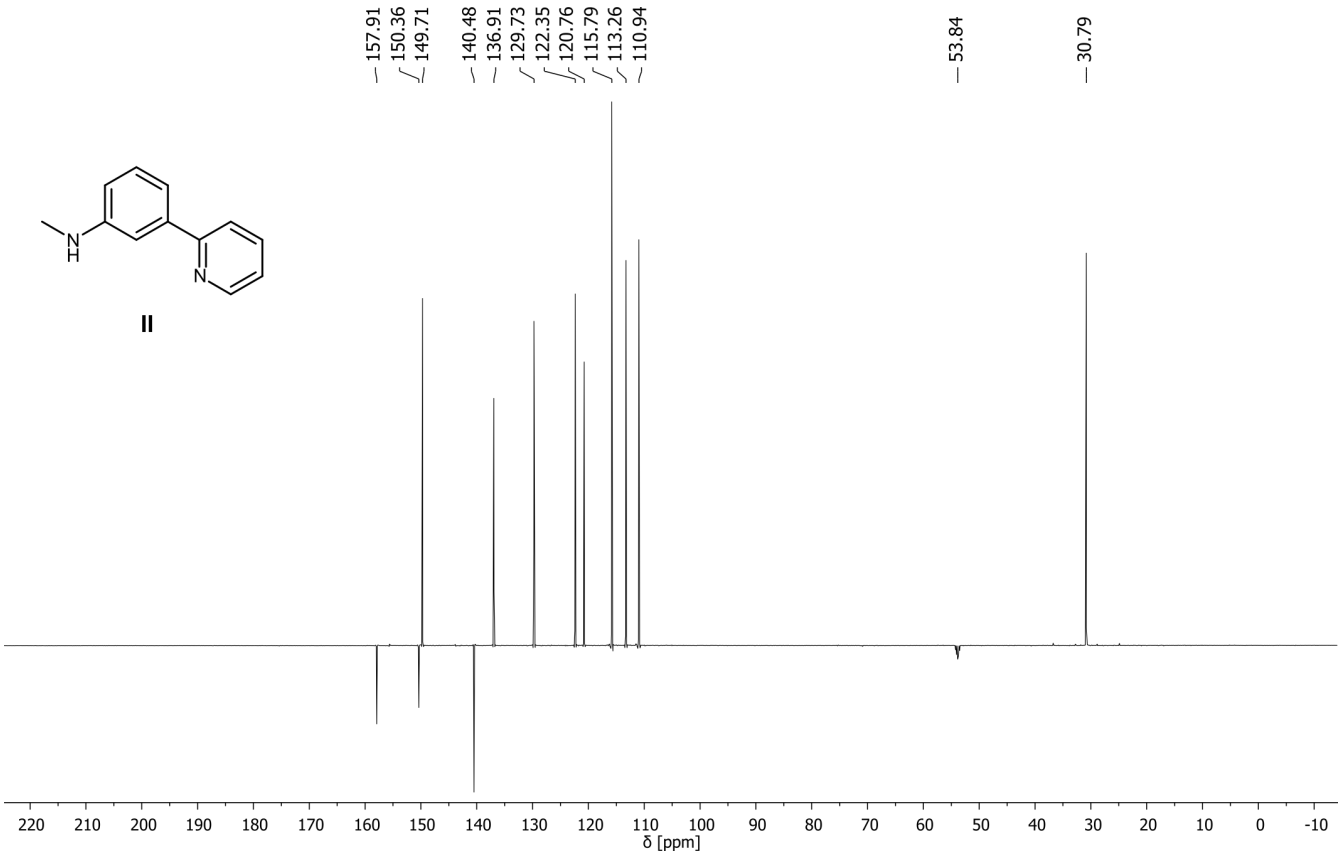

Figure S2. ^{13}C{^{1}H} (151 MHz, CD_2Cl_2) *N*-methyl-3-(pyridin-2-yl)aniline

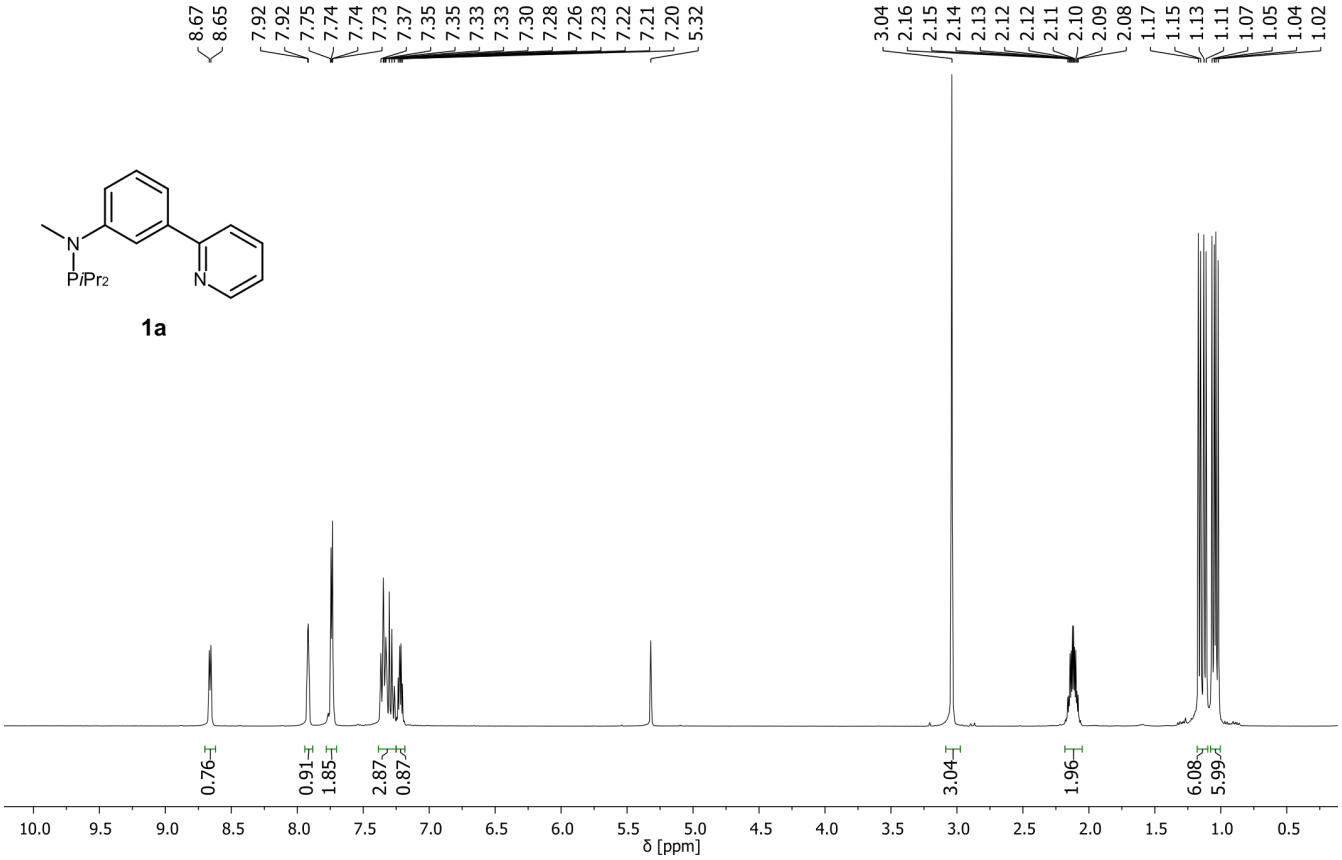

Figure S3. ^{1}H (400 MHz, CD_2Cl_2) $^{i\mathrm{Pr}}$PCN^{NMe}

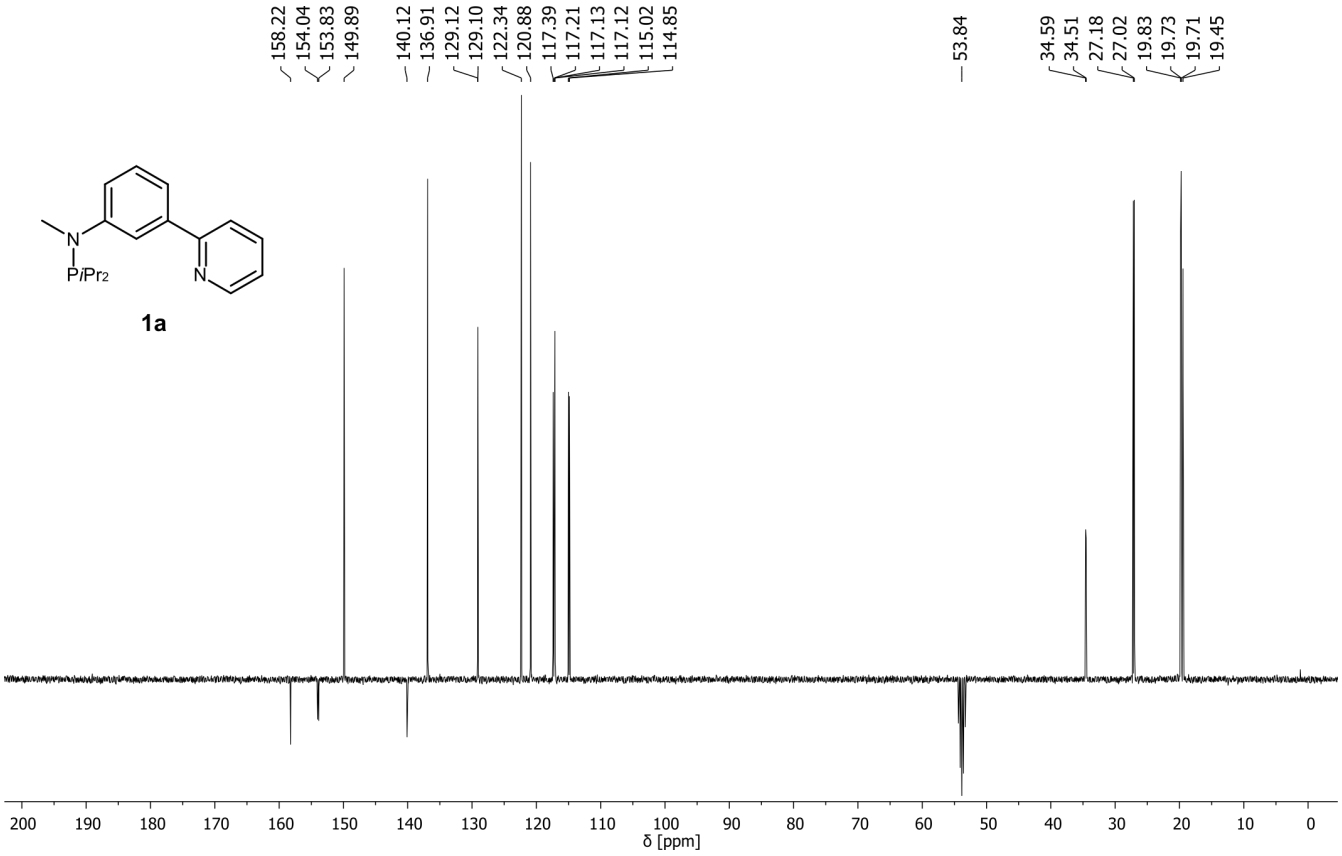

Figure S4. ^{13}C{^{1}H} (101 MHz, CD_2Cl_2) $^{i\mathrm{Pr}}$PCN^{NMe}

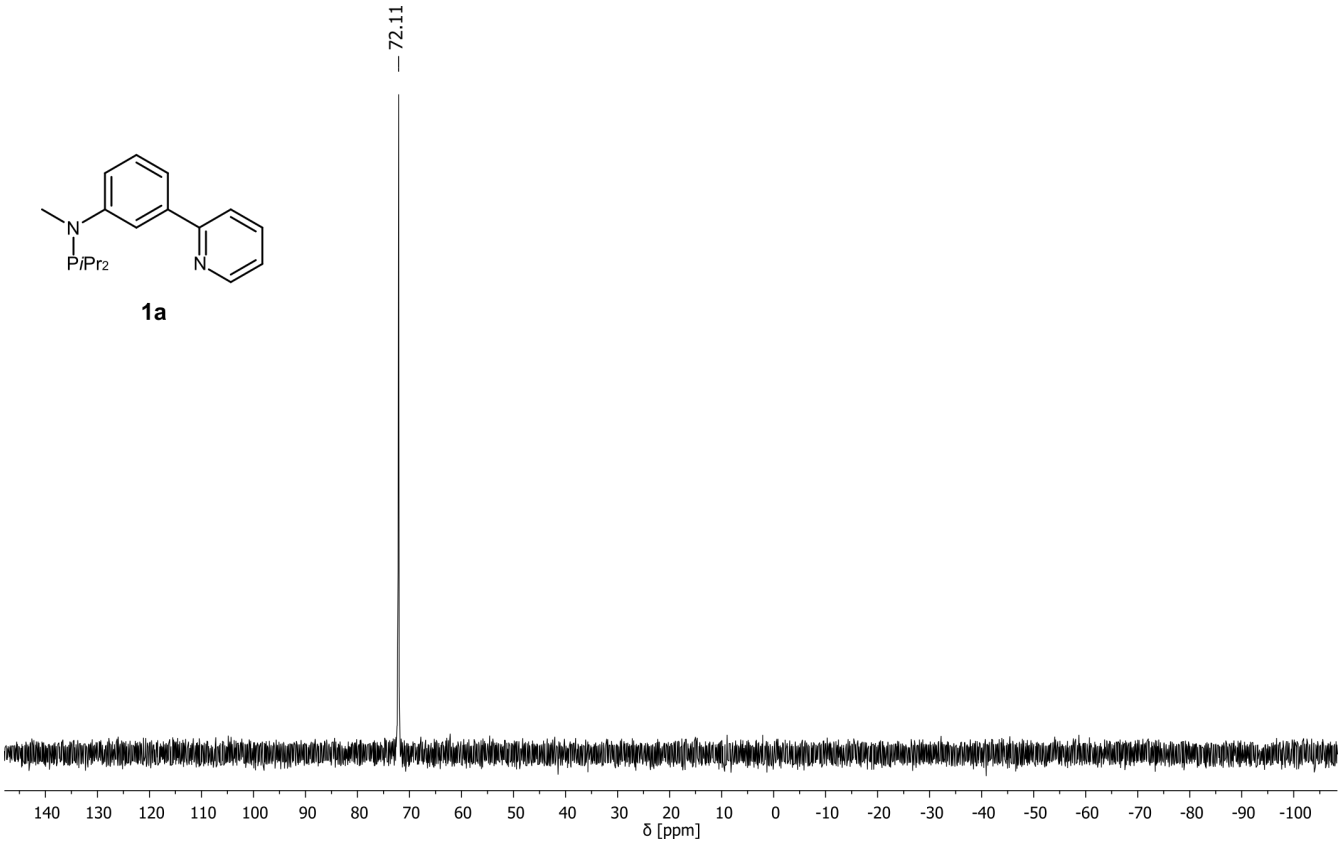

Figure S5. $^{31}P\{^{1}H\}$ (162 MHz, CD_2Cl_2) $^{iPr}PCN^{NMe}$

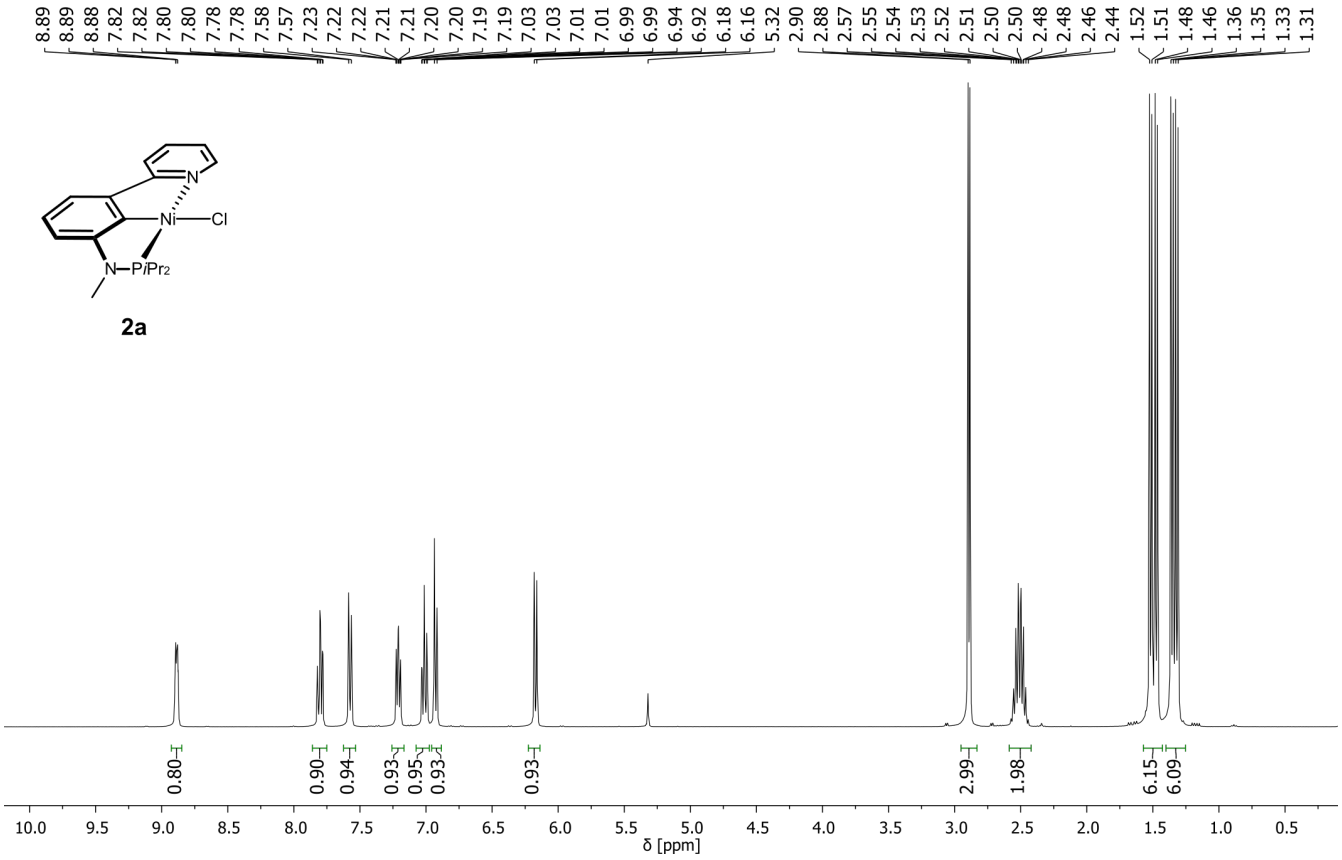

Figure S6. ^{1}H (400 MHz, CD_2Cl_2) [Ni($^{iPr}PCN^{NMe}$)Cl]

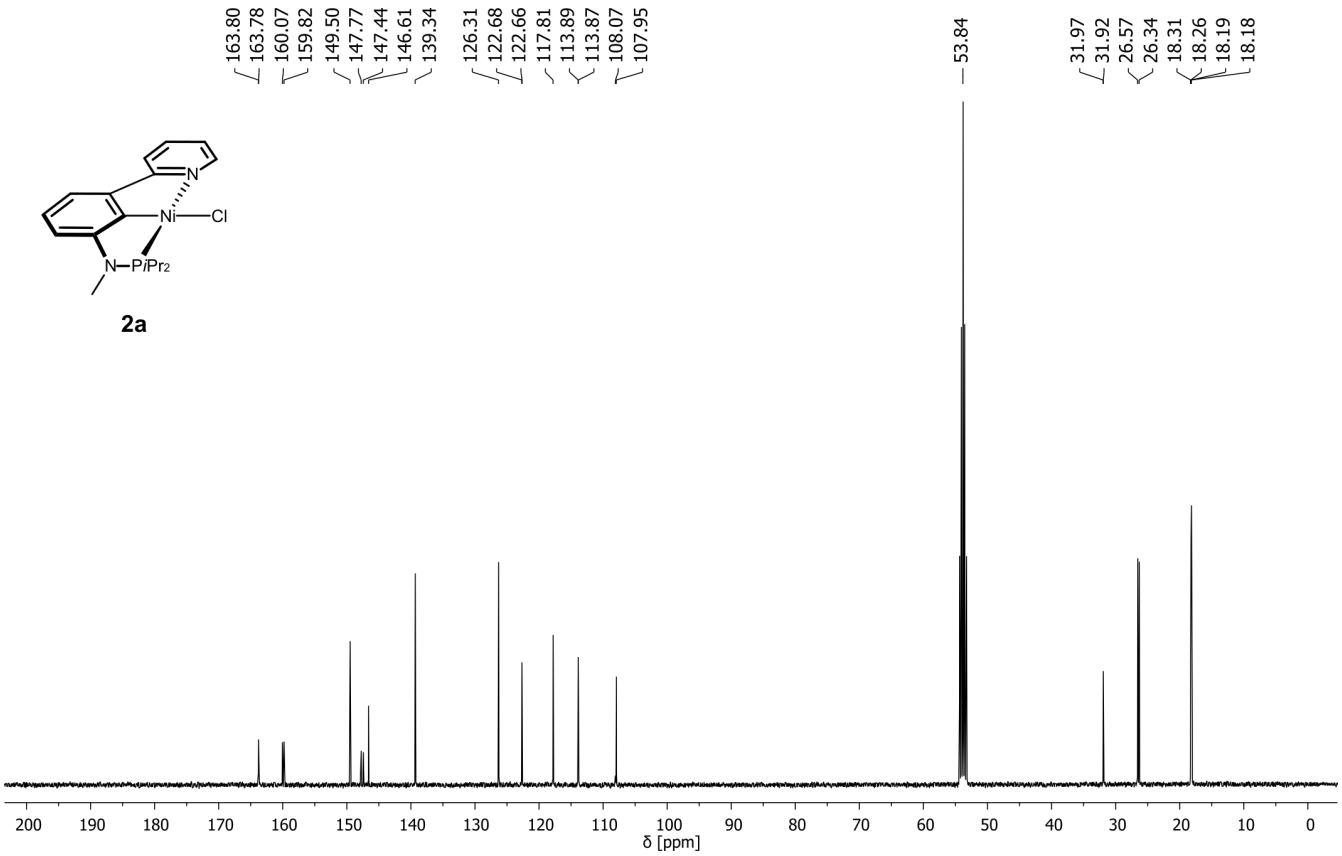

Figure S7. $^{13}C\{^{1}H\}$ (101 MHz, CD_2Cl_2) [Ni(^{iPr}PCN^{NMe})Cl]

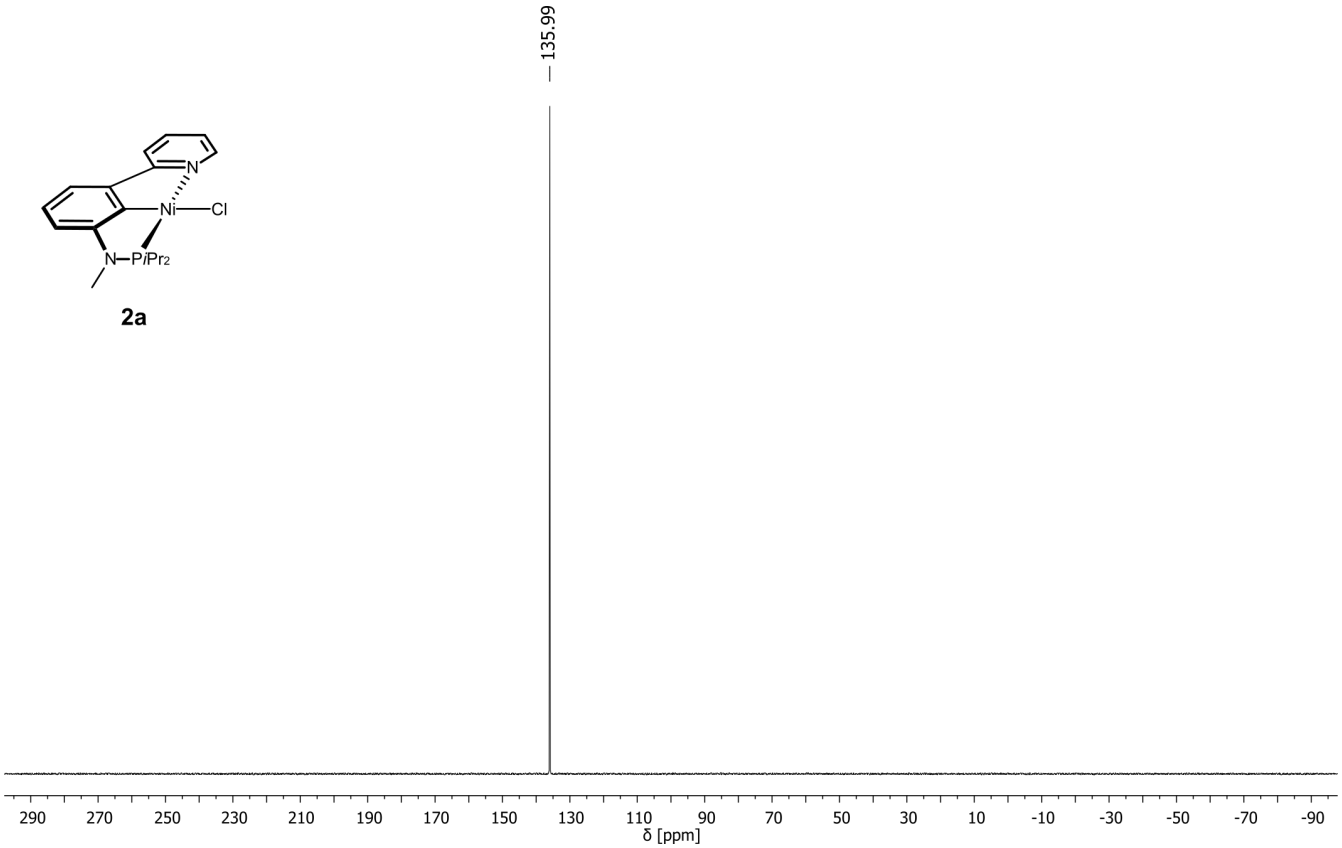

Figure S8. $^{31}P\{^{1}H\}$ (162 MHz, CD_2Cl_2) [Ni(^{iPr}PCN^{NMe})Cl]

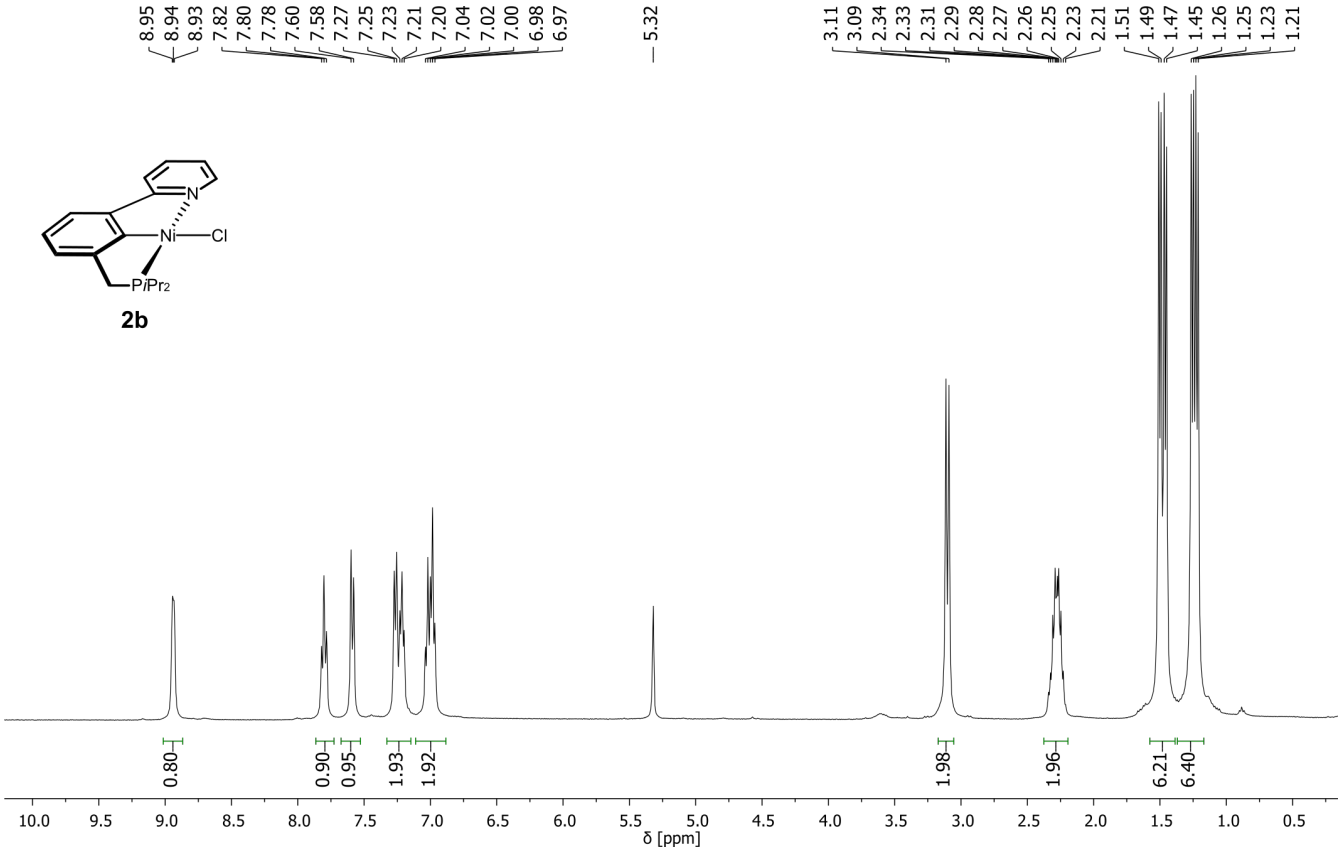

Figure S9. ^{1}H (400 MHz, CD_2Cl_2) [Ni(^{iPr}PCN^{CH_2})Cl]

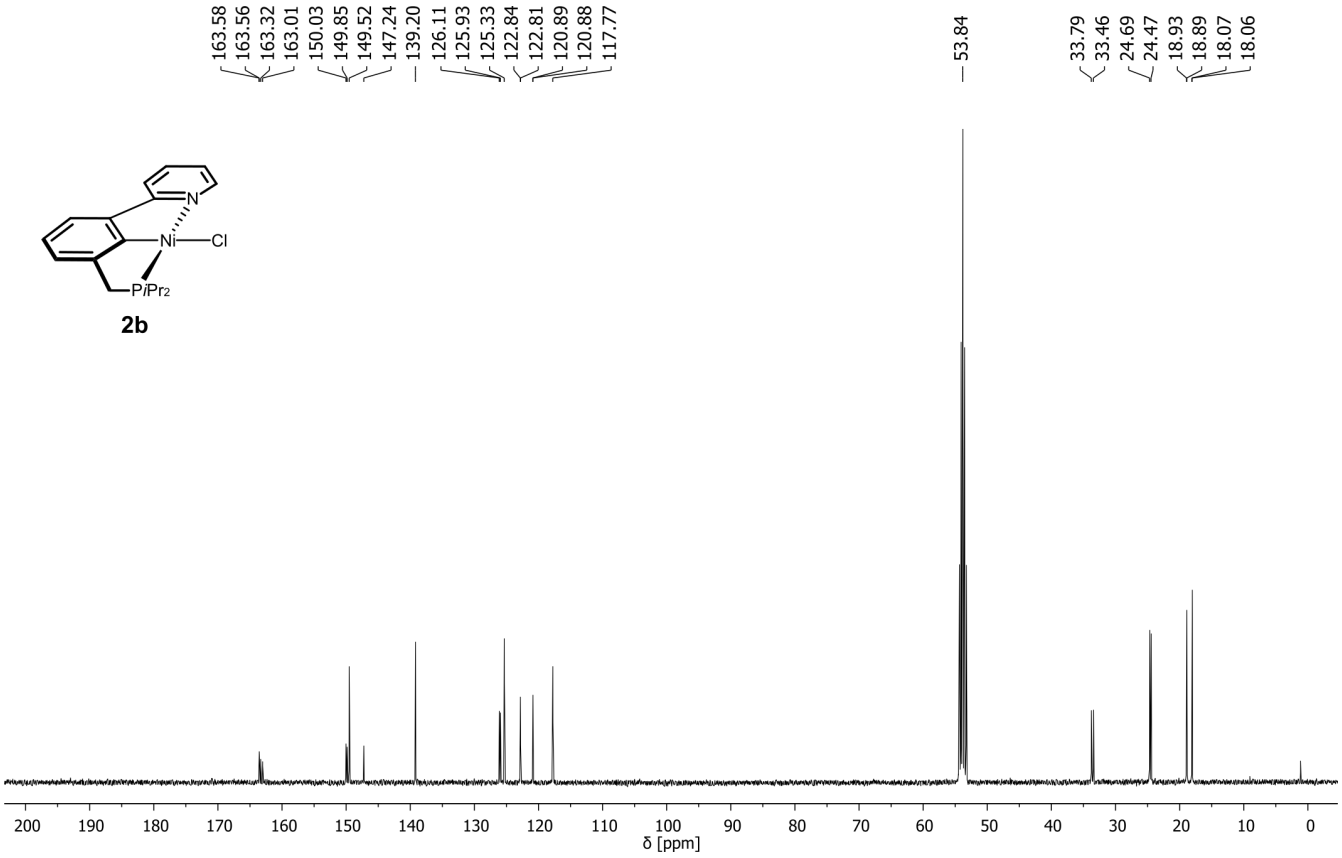

Figure S10. ^{13}C{^{1}H} (101 MHz, CD_2Cl_2) [Ni(^{iPr}PCN^{CH_2})Cl]

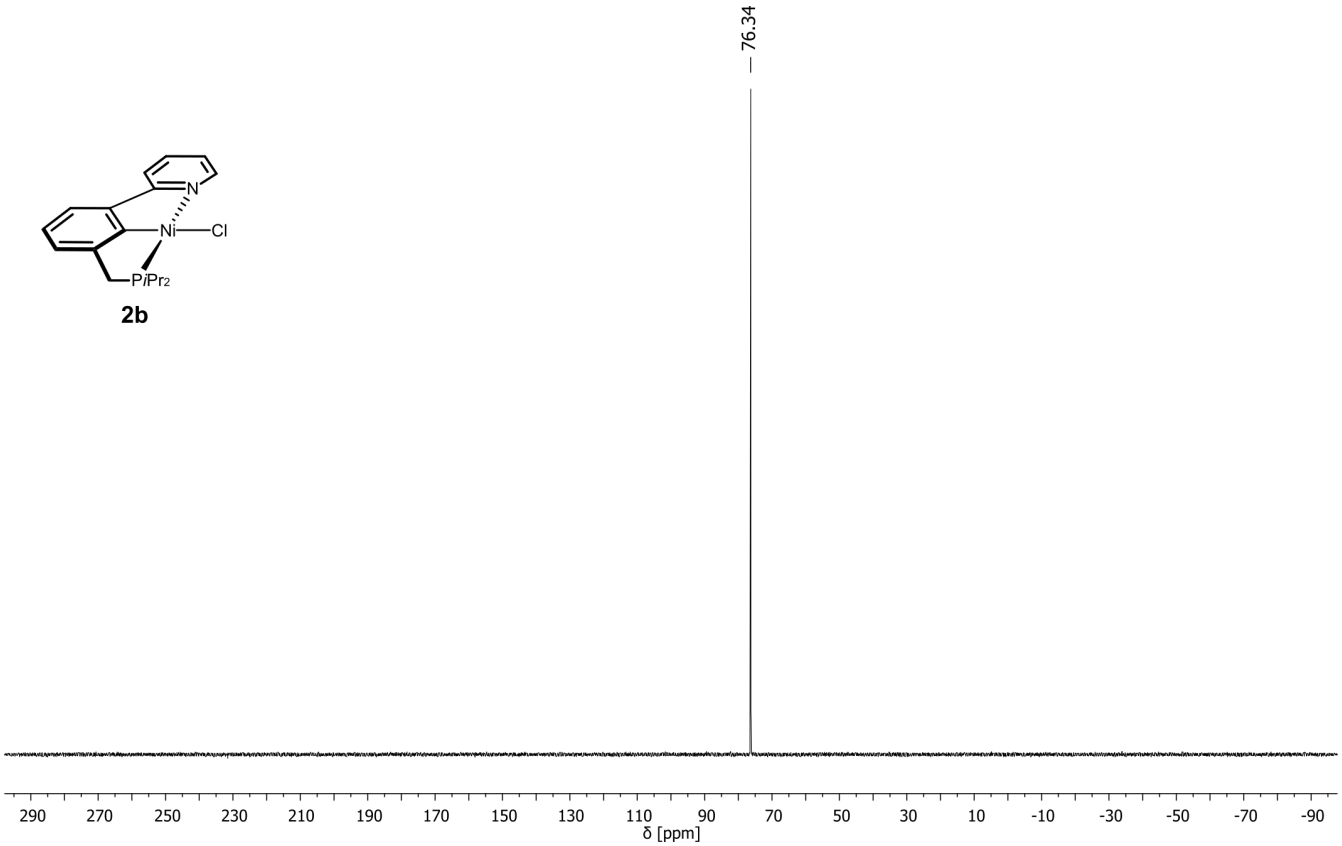

Figure S11. $^{31}P\{^{1}H\}$ (162 MHz, CD_2Cl_2) [Ni(^{iPr}PCN^{CH_2})Cl]

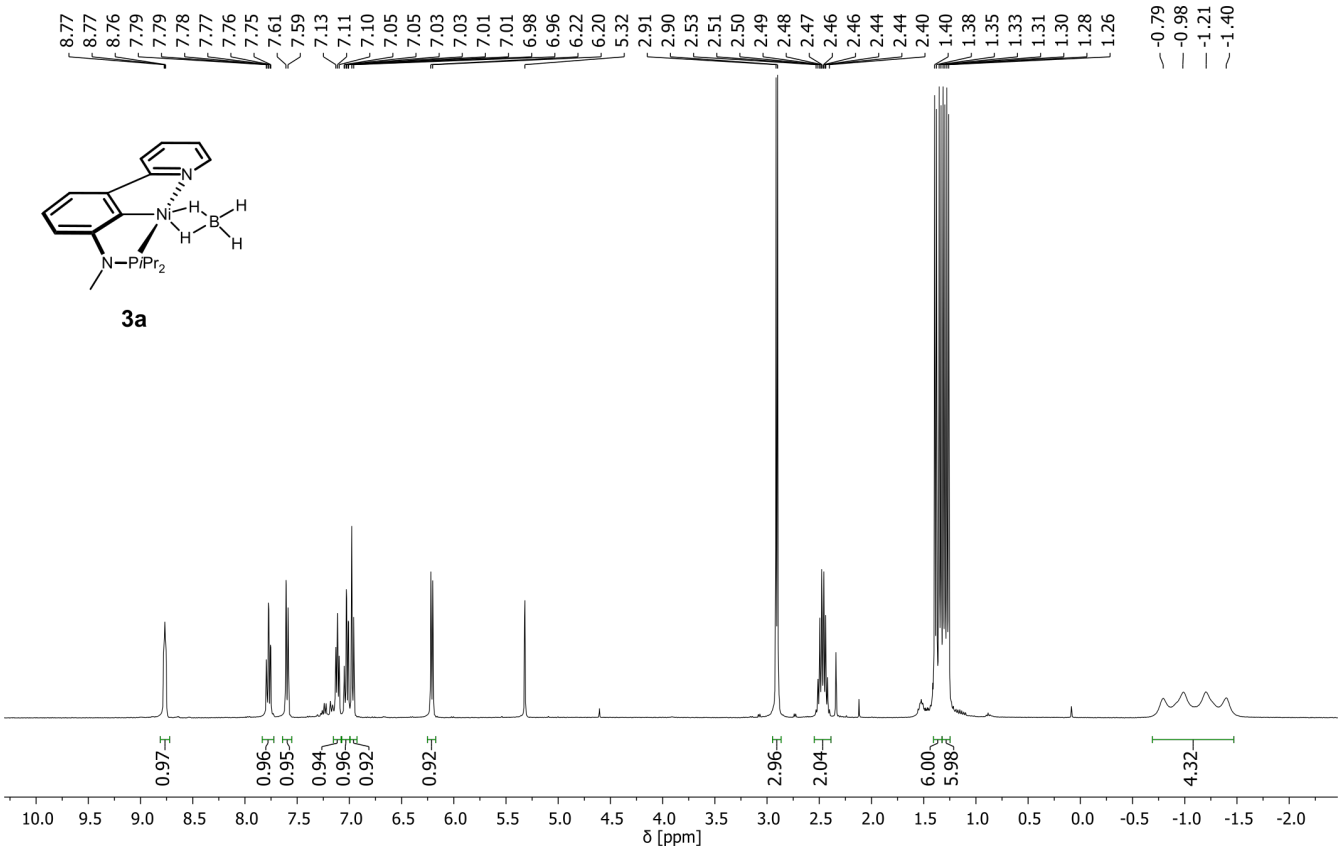

Figure S12. ^{1}H (400 MHz, CD_2Cl_2) [Ni(^{iPr}PCN^{NMe})(η^2-BH_4)]

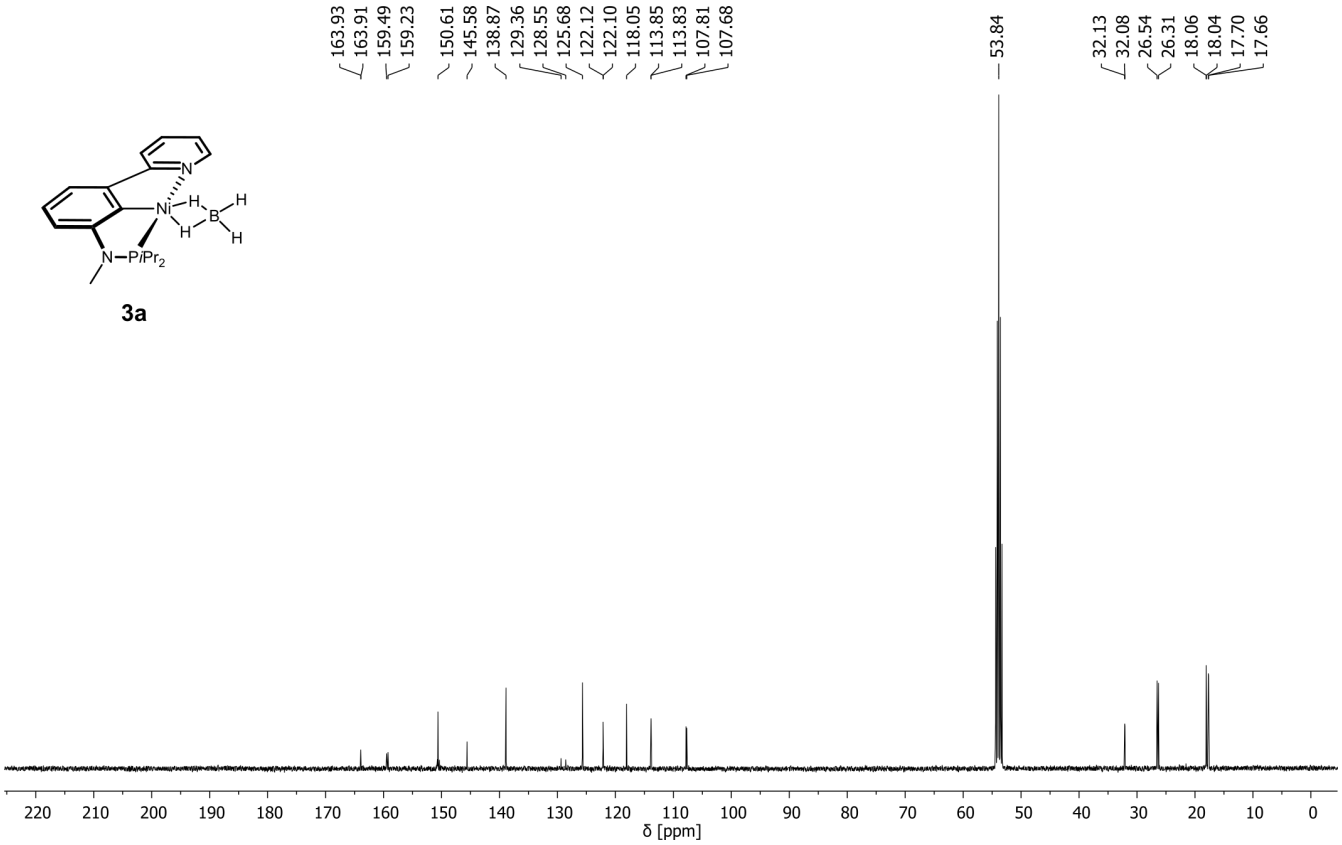

Figure S13. $^{13}C\{^{1}H\}$ (101 MHz, CD_2Cl_2) [Ni(^{iPr}PCN^{NMe})(η^2-BH_4)]

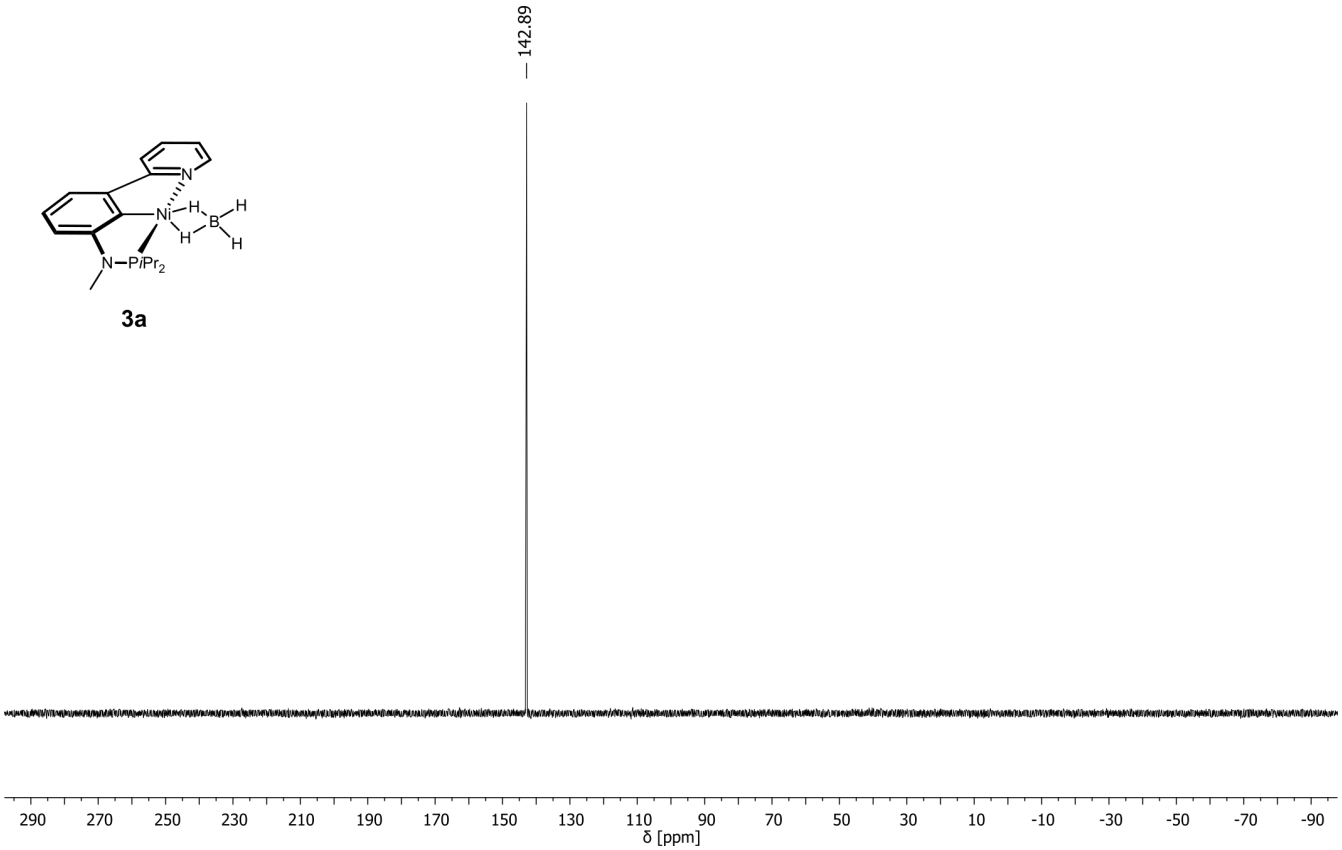

Figure S14. $^{31}P\{^{1}H\}$ (162 MHz, CD_2Cl_2) [Ni(^{iPr}PCN^{NMe})(η^2-BH_4)]

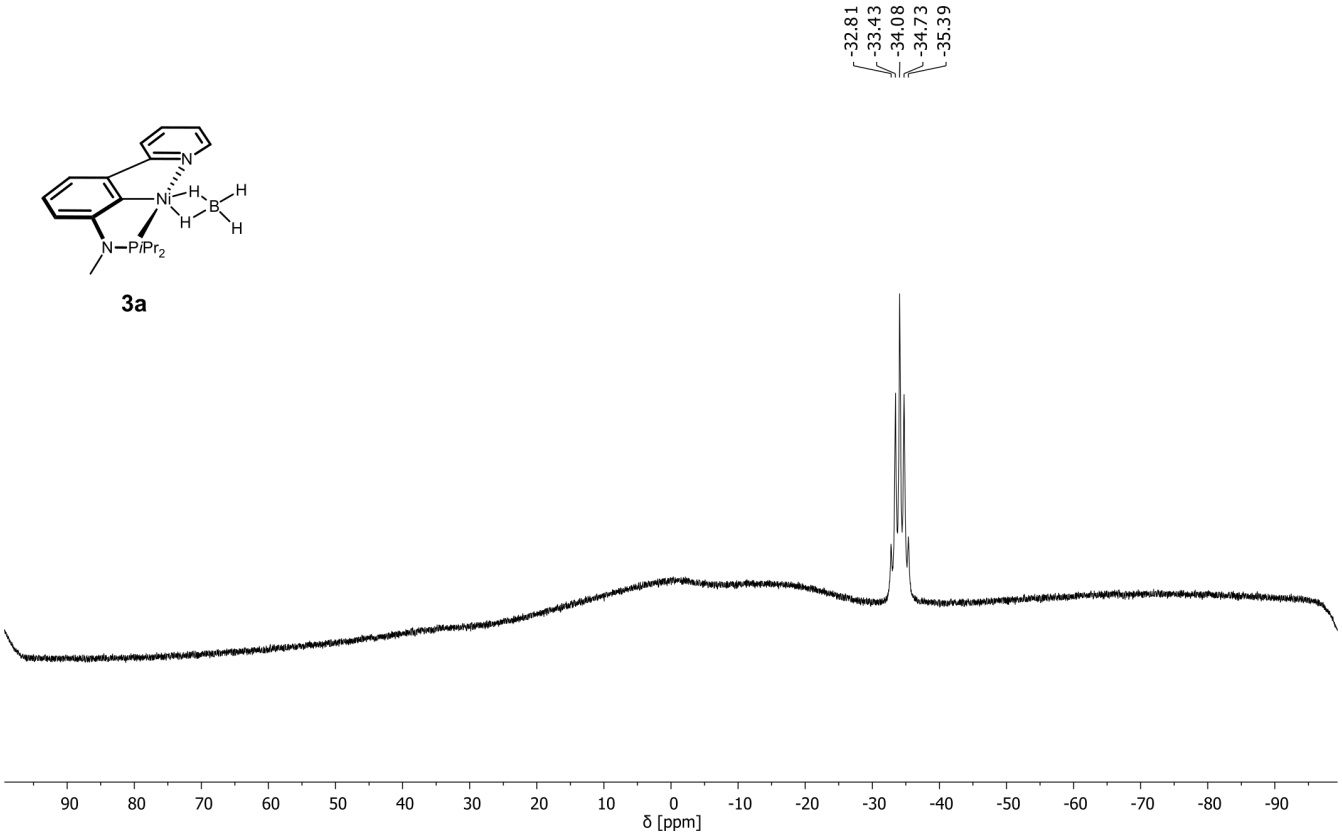

Figure S15. ^{11}B no decoupling (128 MHz, CD_2Cl_2) [Ni($^{i\mathrm{Pr}}$PCN^{NMe})(η^2-BH_4)]

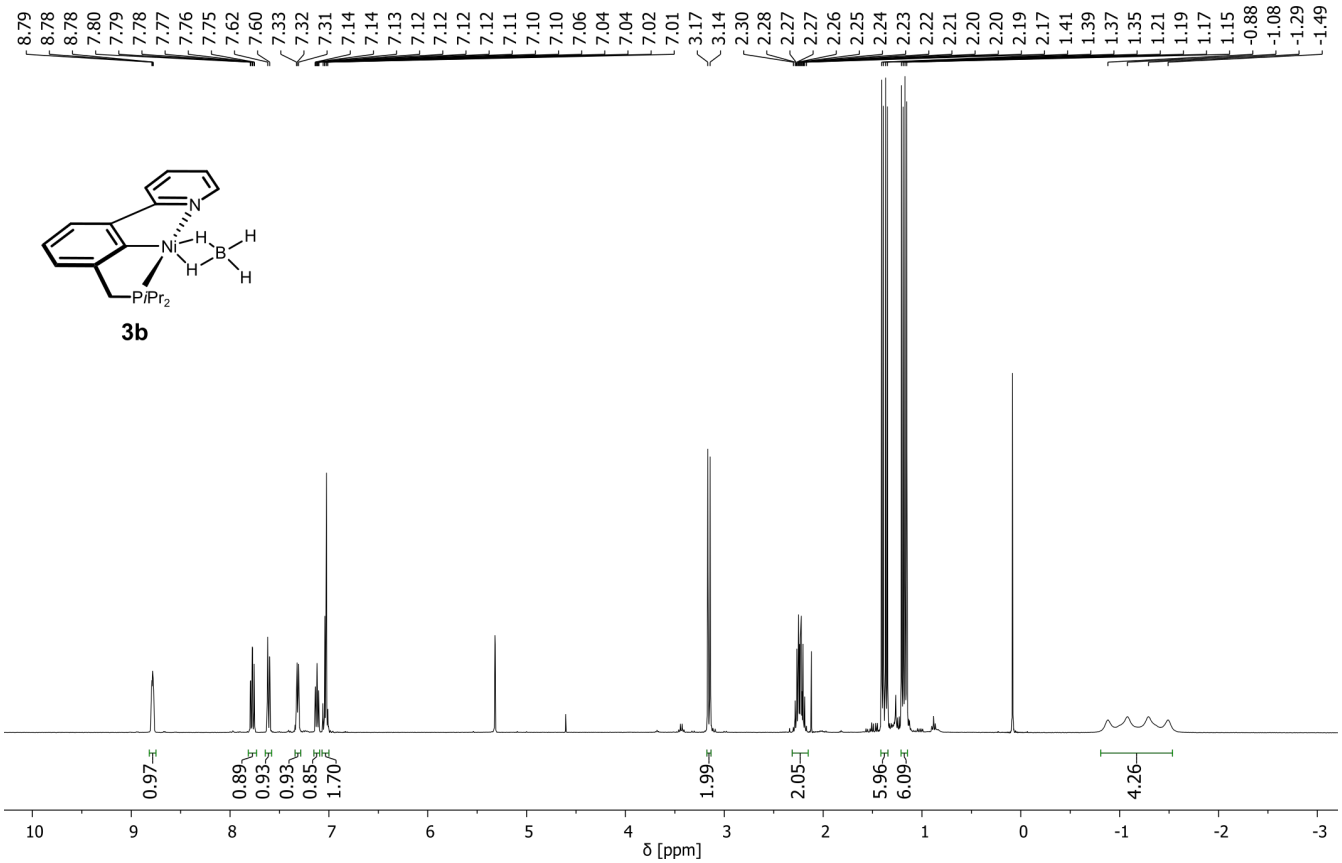

Figure S16. ^{1}H (400 MHz, CD_2Cl_2) [Ni($^{i\mathrm{Pr}}$PCN$^{\mathrm{CH_2}}$)(η^2-BH_4)]

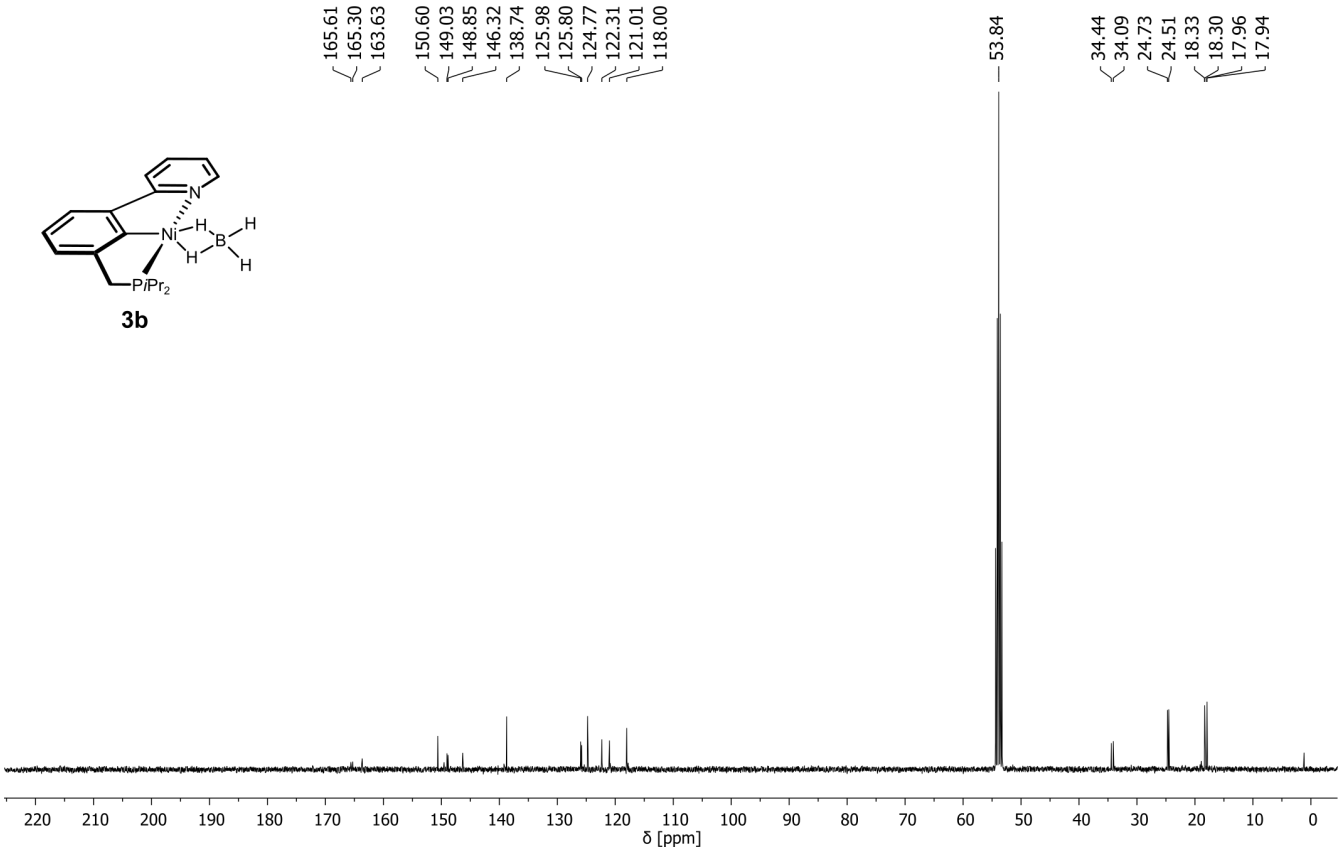

Figure S17. $^{13}C\{^1H\}$ (101 MHz, CD_2Cl_2) [Ni($^{i\mathrm{Pr}}$PCN$^{\mathrm{CH_2}}$)(η^2-BH_4)]

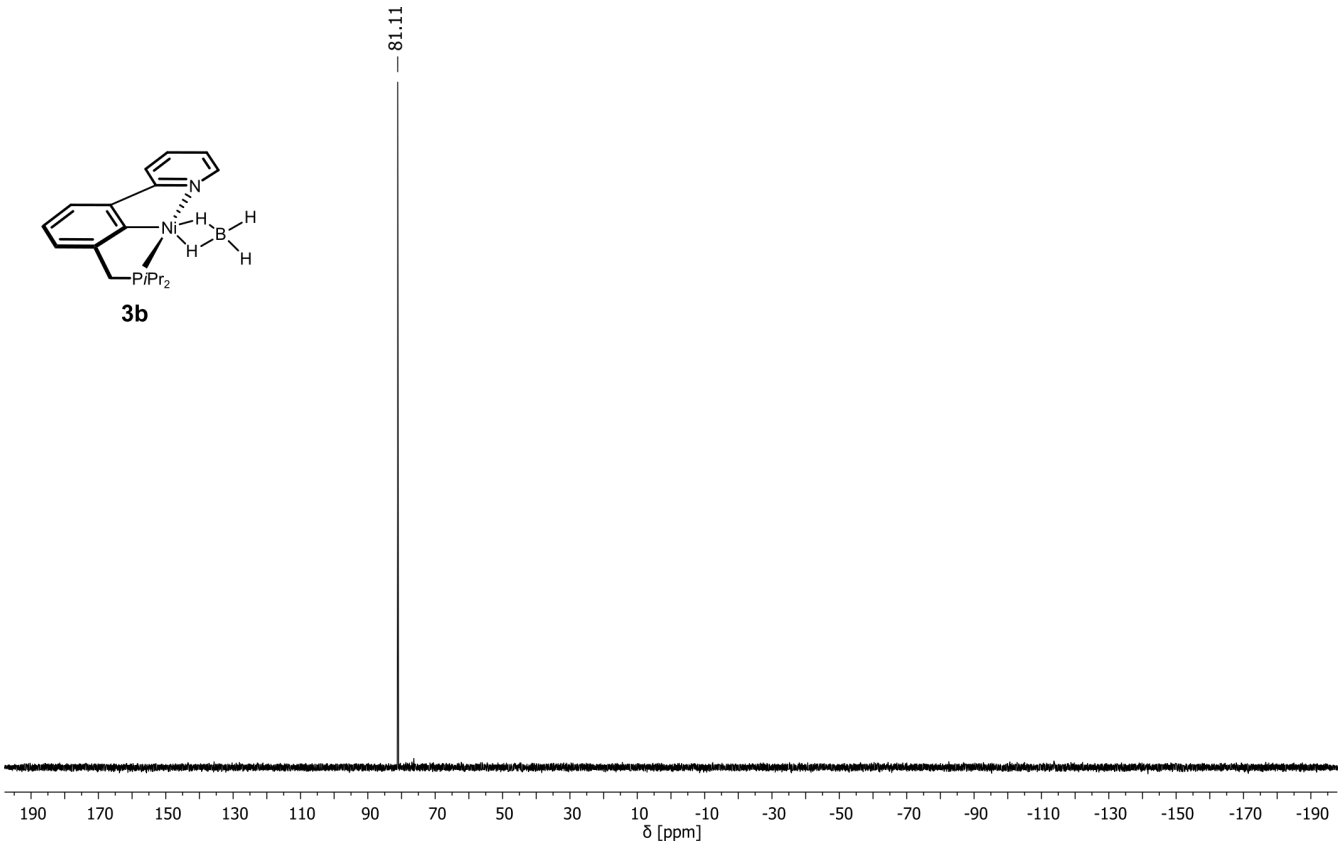

Figure S18. $^{31}P\{^1H\}$ (162 MHz, CD_2Cl_2) [Ni($^{i\mathrm{Pr}}$PCN$^{\mathrm{CH_2}}$)(η^2-BH_4)]

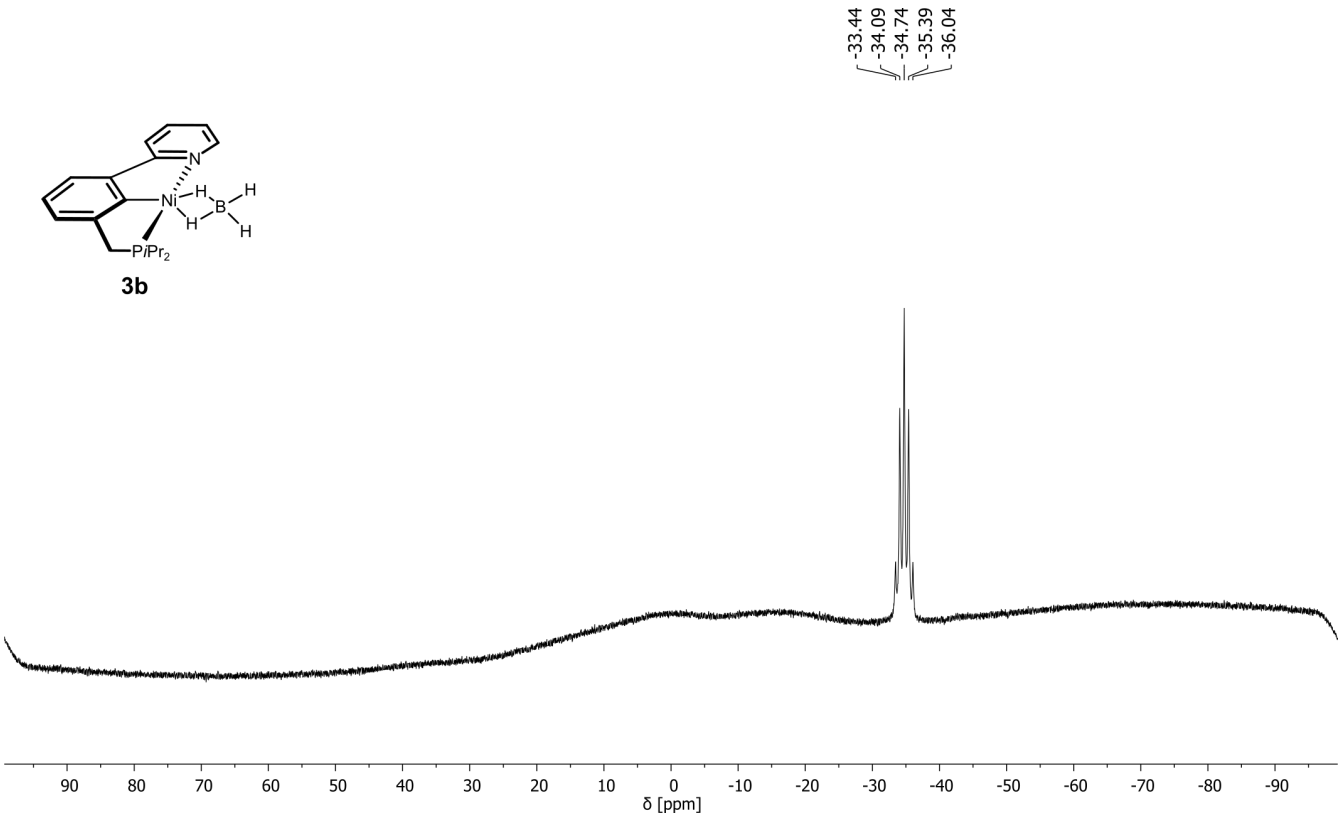

Figure S19. ^{11}B no decoupling (128 MHz, CD_2Cl_2) [Ni(^{iPr}PCN^{CH_2})(η^2-BH_4)]

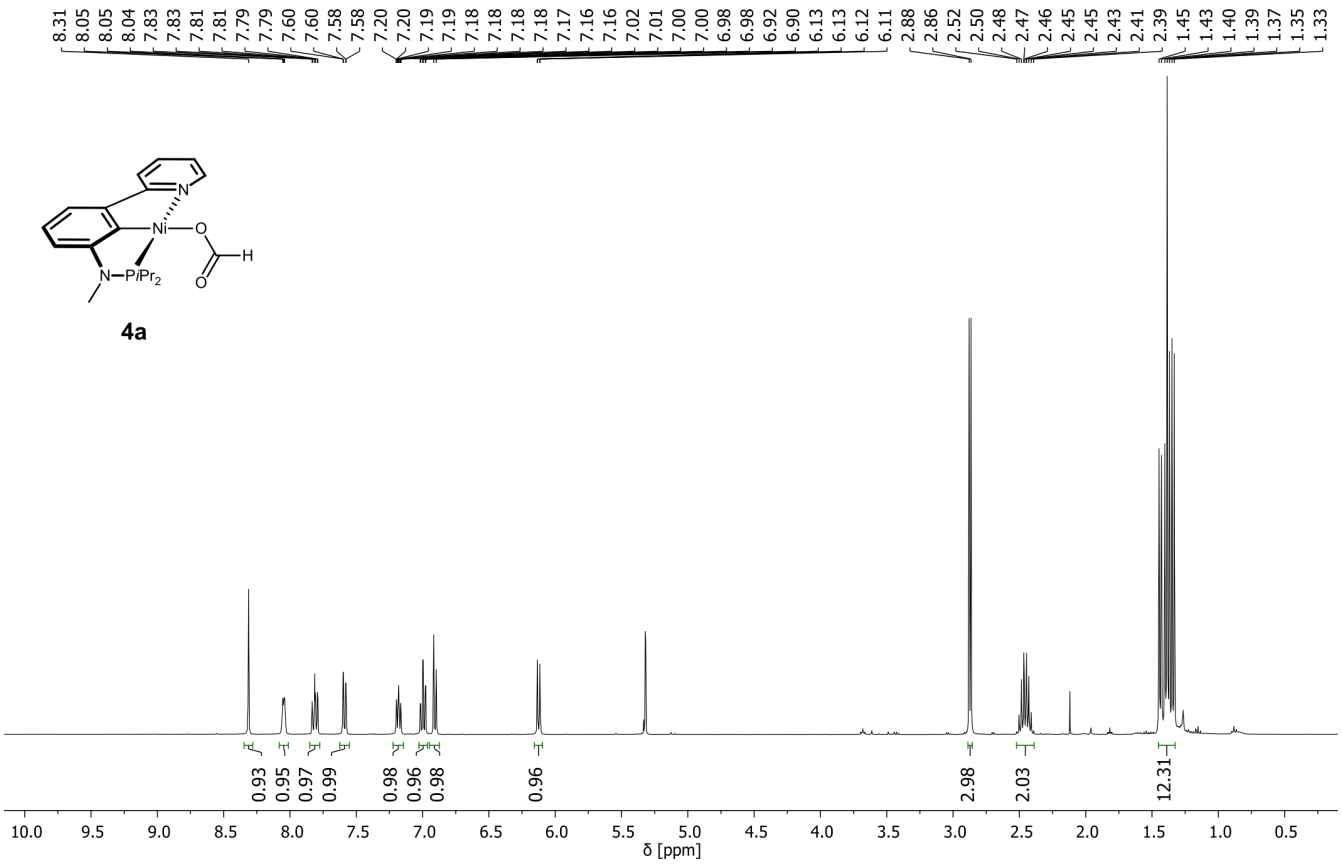

Figure S20. ^{1}H (400 MHz, CD_2Cl_2) [Ni(^{iPr}PCN^{NMe})(OCHO)]

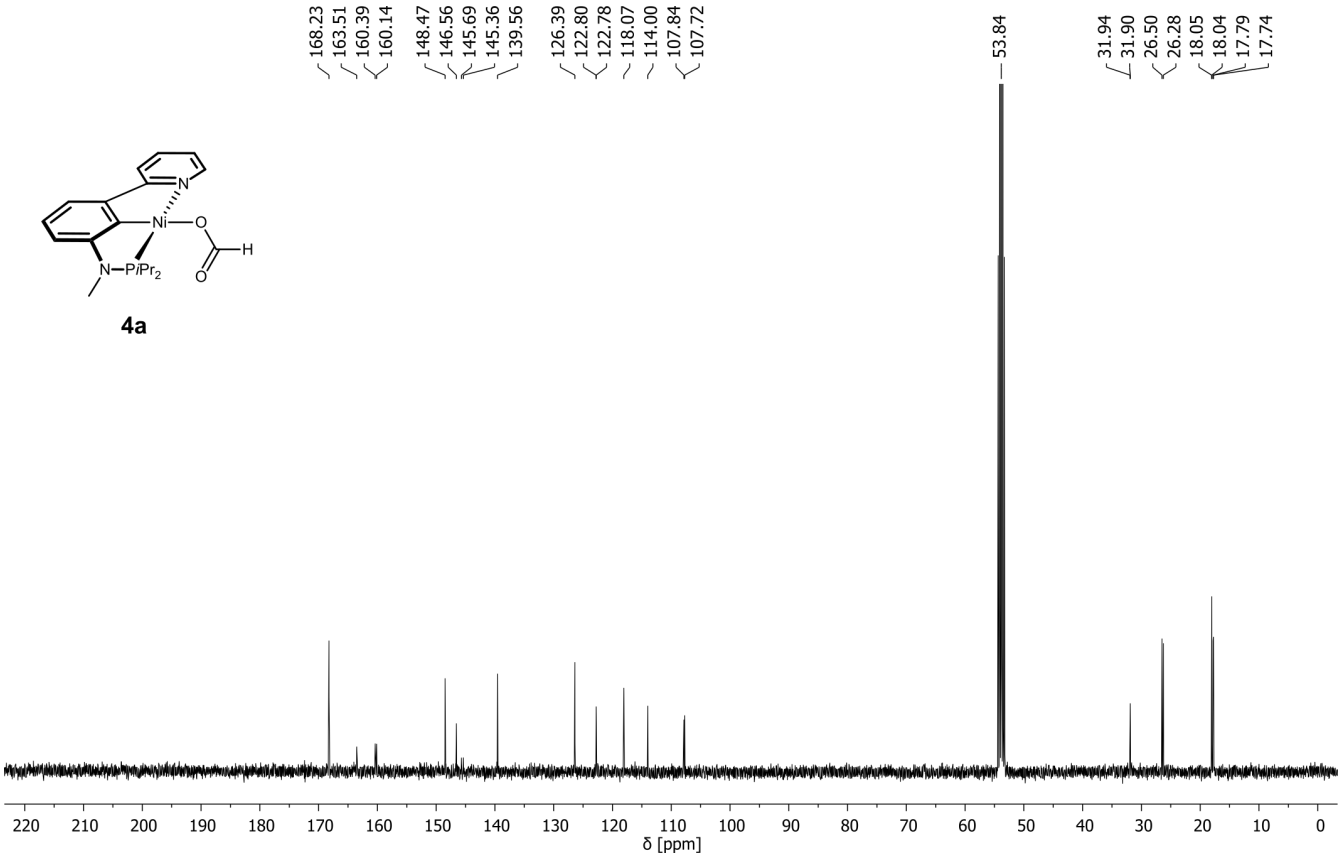

Figure S21. $^{13}C\{^{1}H\}$ (101 MHz, CD_2Cl_2) [Ni(^{iPr}PCN^{NMe})(OCHO)]

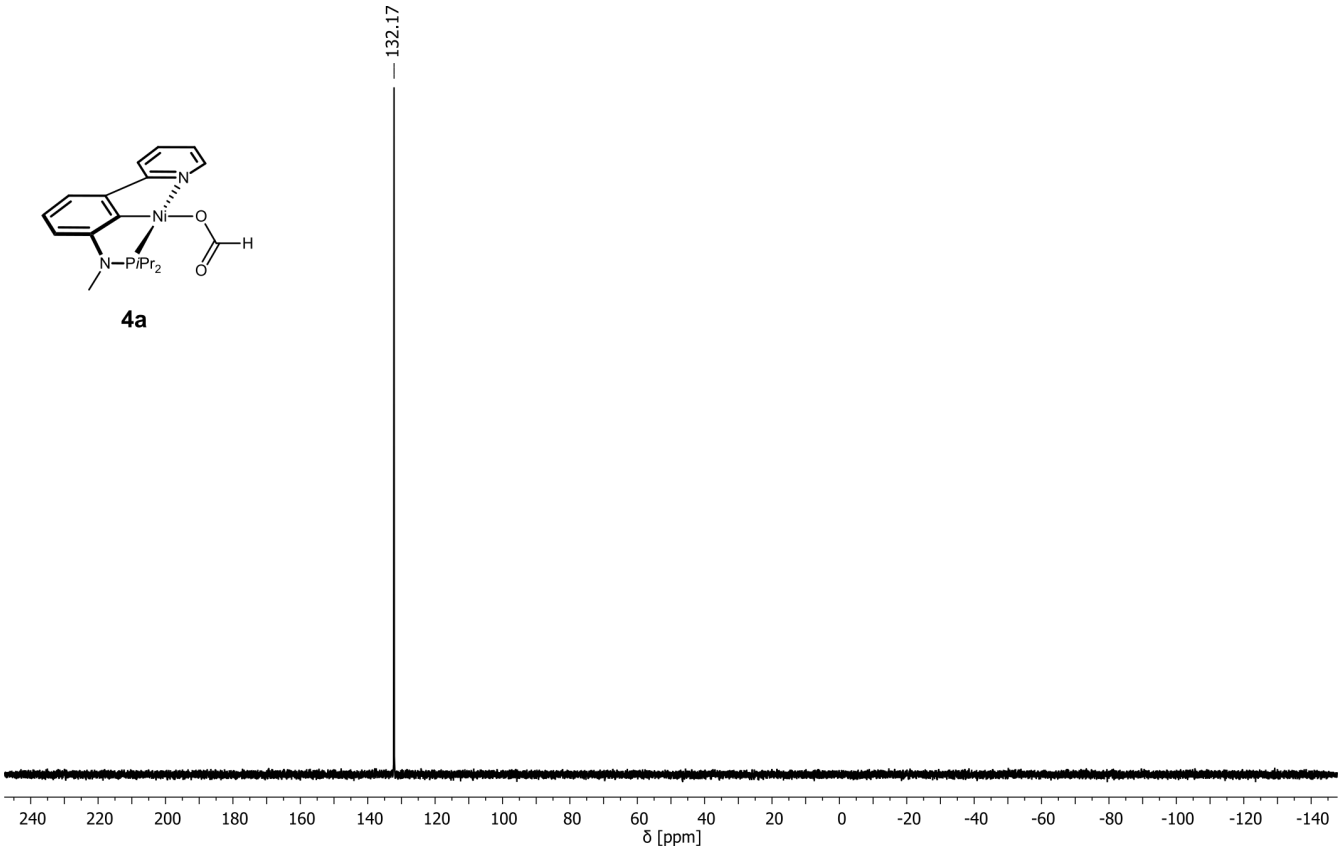

Figure S22. $^{31}P\{^{1}H\}$ (162 MHz, CD_2Cl_2) [Ni(^{iPr}PCN^{NMe})(OCHO)]

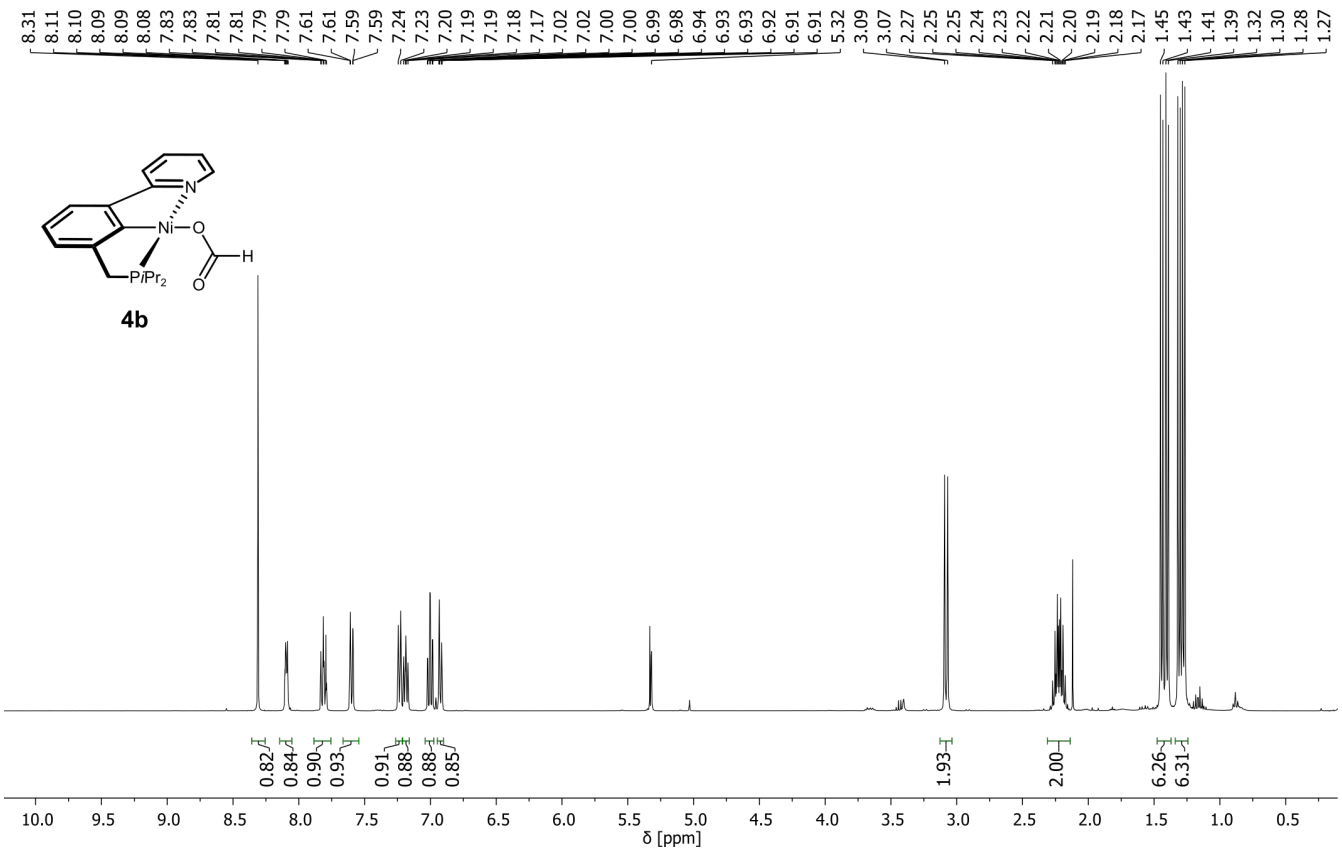

Figure S23. ^{1}H (400 MHz, CD_2Cl_2) [Ni($^{i\mathrm{Pr}}$PCN$^{\mathrm{CH_2}}$)(OCHO)]

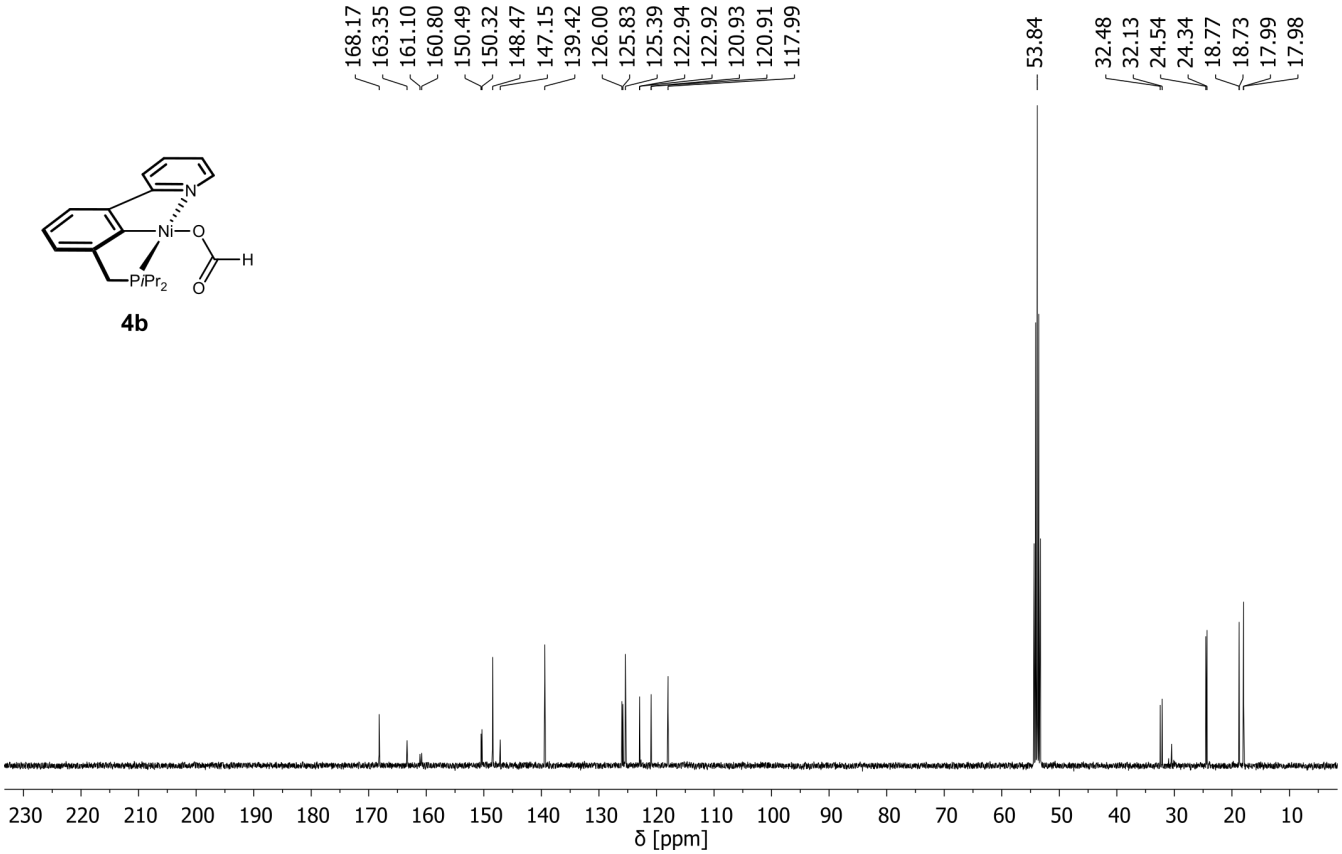

Figure S24. ^{13}C{^{1}H} (101 MHz, CD_2Cl_2) [Ni($^{i\mathrm{Pr}}$PCN$^{\mathrm{CH_2}}$)(OCHO)]

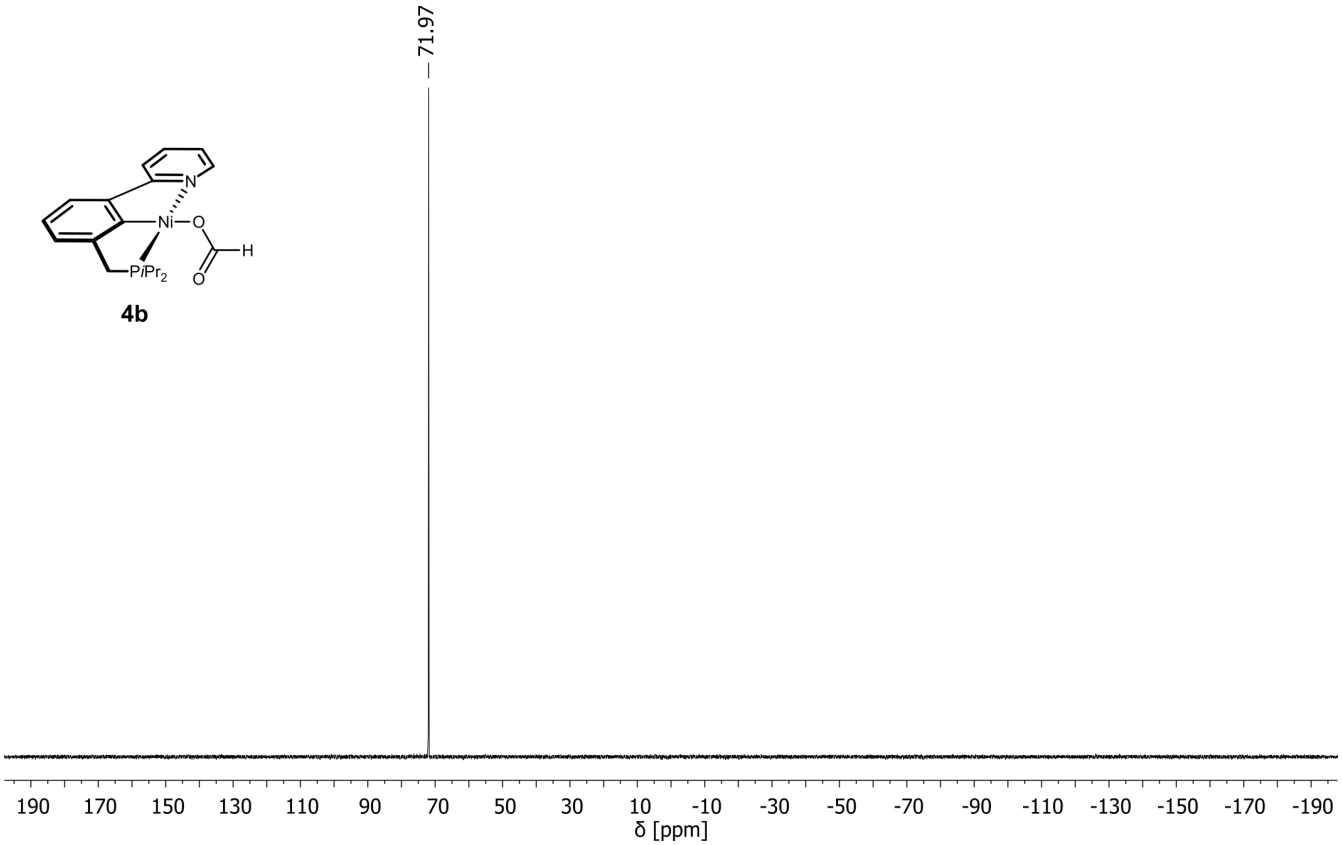

Figure S25. $^{31}P\{^{1}H\}$ (162 MHz, CD_2Cl_2) [Ni(^{iPr}PCN^{CH_2})(OCHO)]

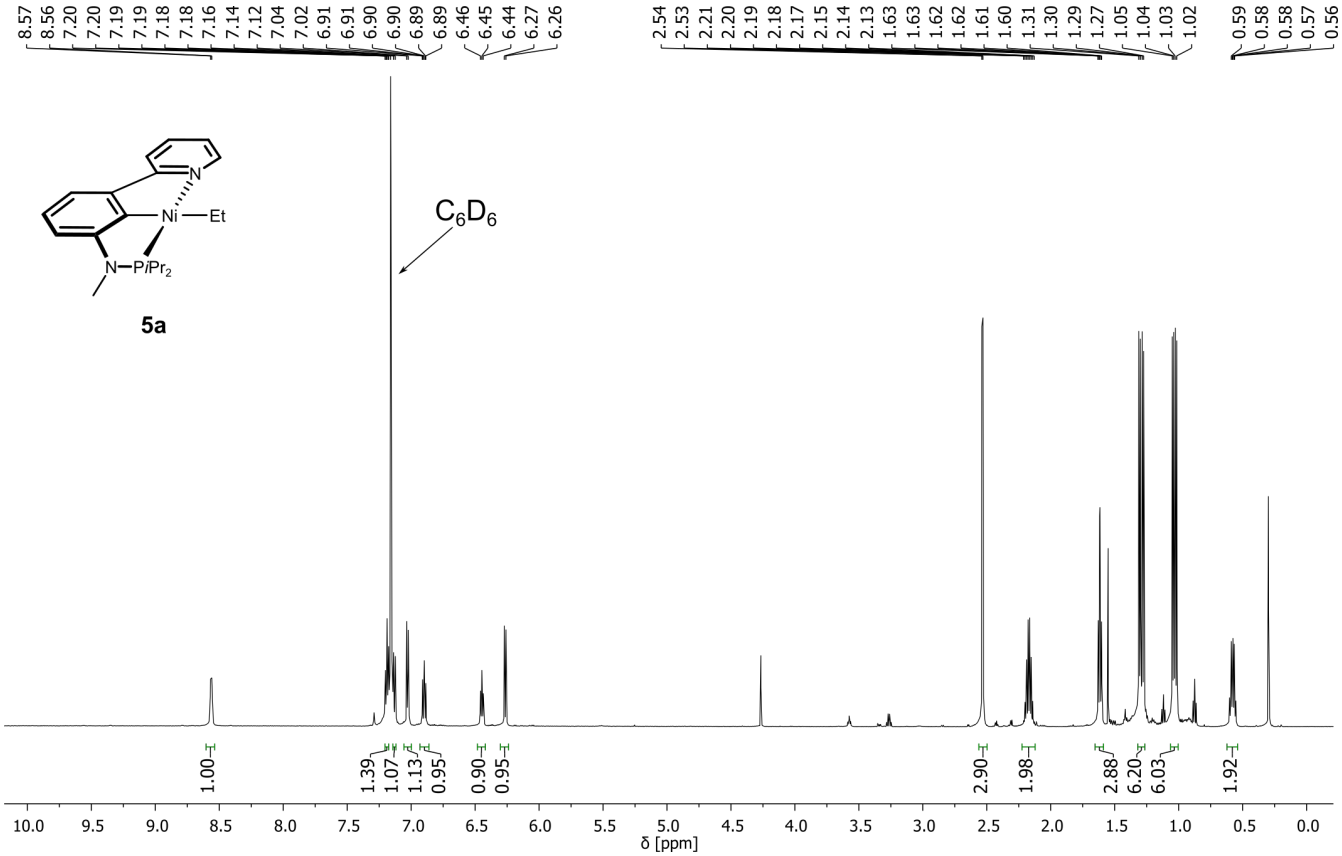

Figure S26. ^{1}H (600 MHz, C_6D_6) [Ni(^{iPr}PCN^{NMe})(η^2-Et)]

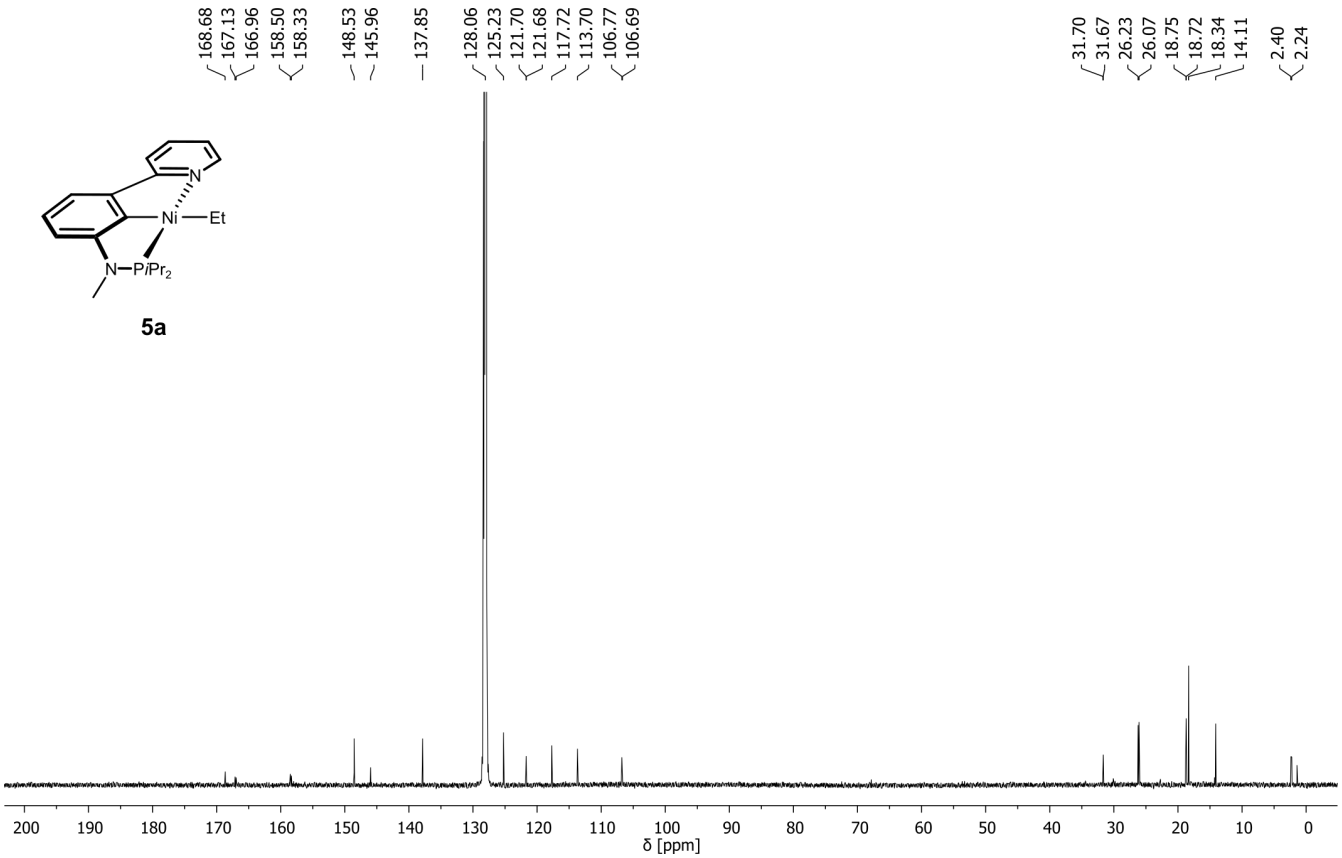

Figure S27. $^{13}C\{^1H\}$ (151 MHz, C_6D_6) [Ni(^{iPr}PCN^{NMe})(η^2-Et)]

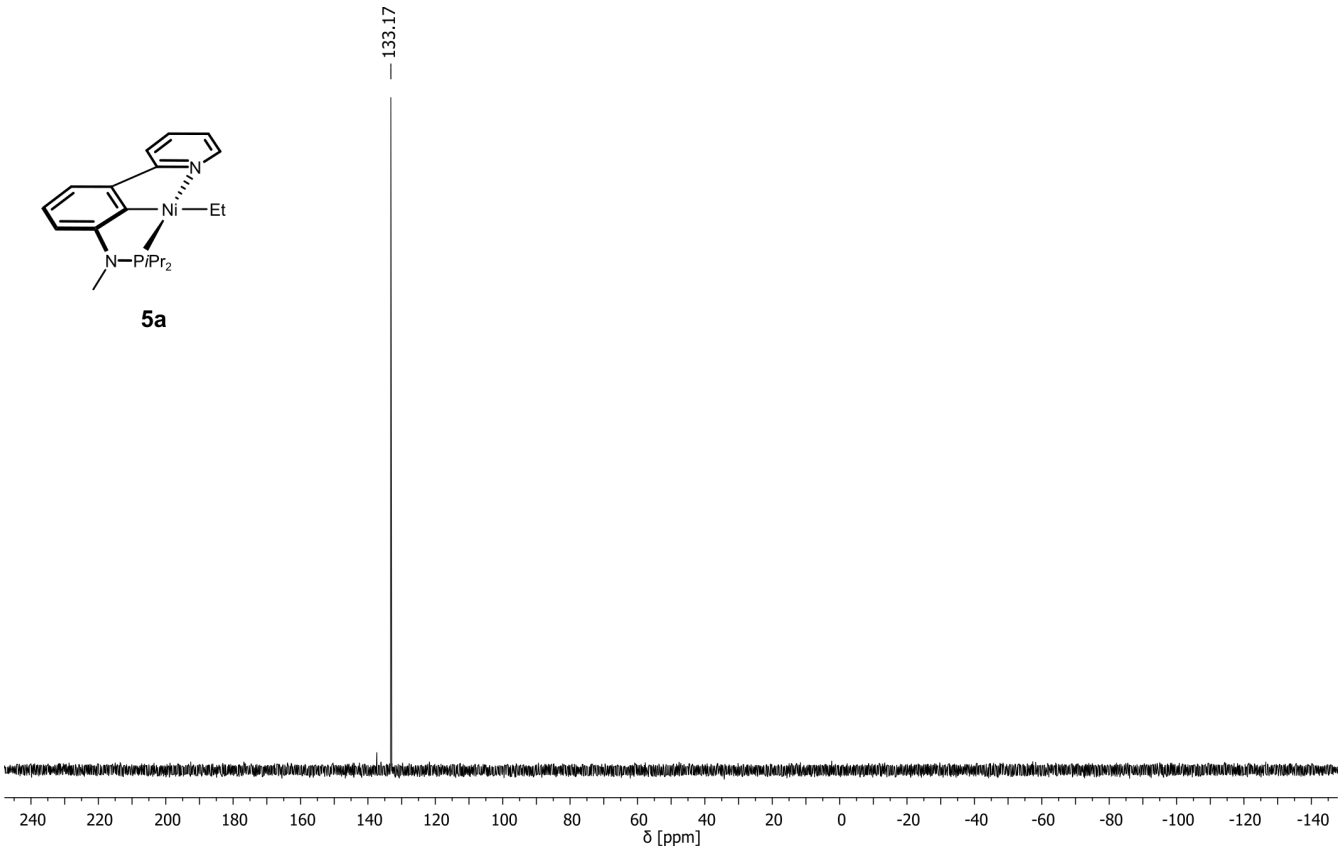

Figure S28. $^{31}P\{^1H\}$ (243 MHz, C_6D_6) [Ni(^{iPr}PCN^{NMe})(η^2-Et)]

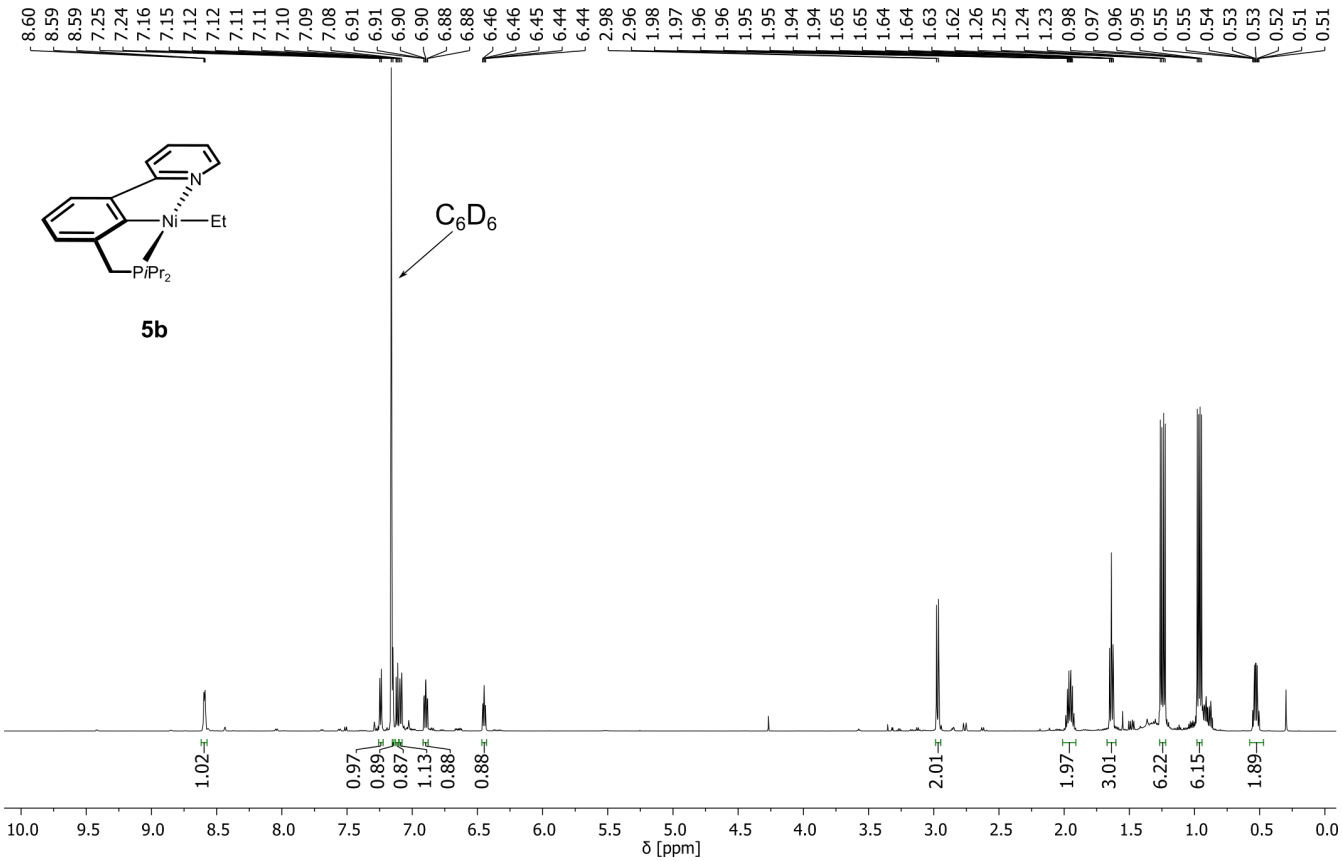

Figure S29. ^{1}H (600 MHz, C_6D_6) [Ni($^{i\mathrm{Pr}}$PCN$^{\mathrm{CH_2}}$)(η^2-Et)]

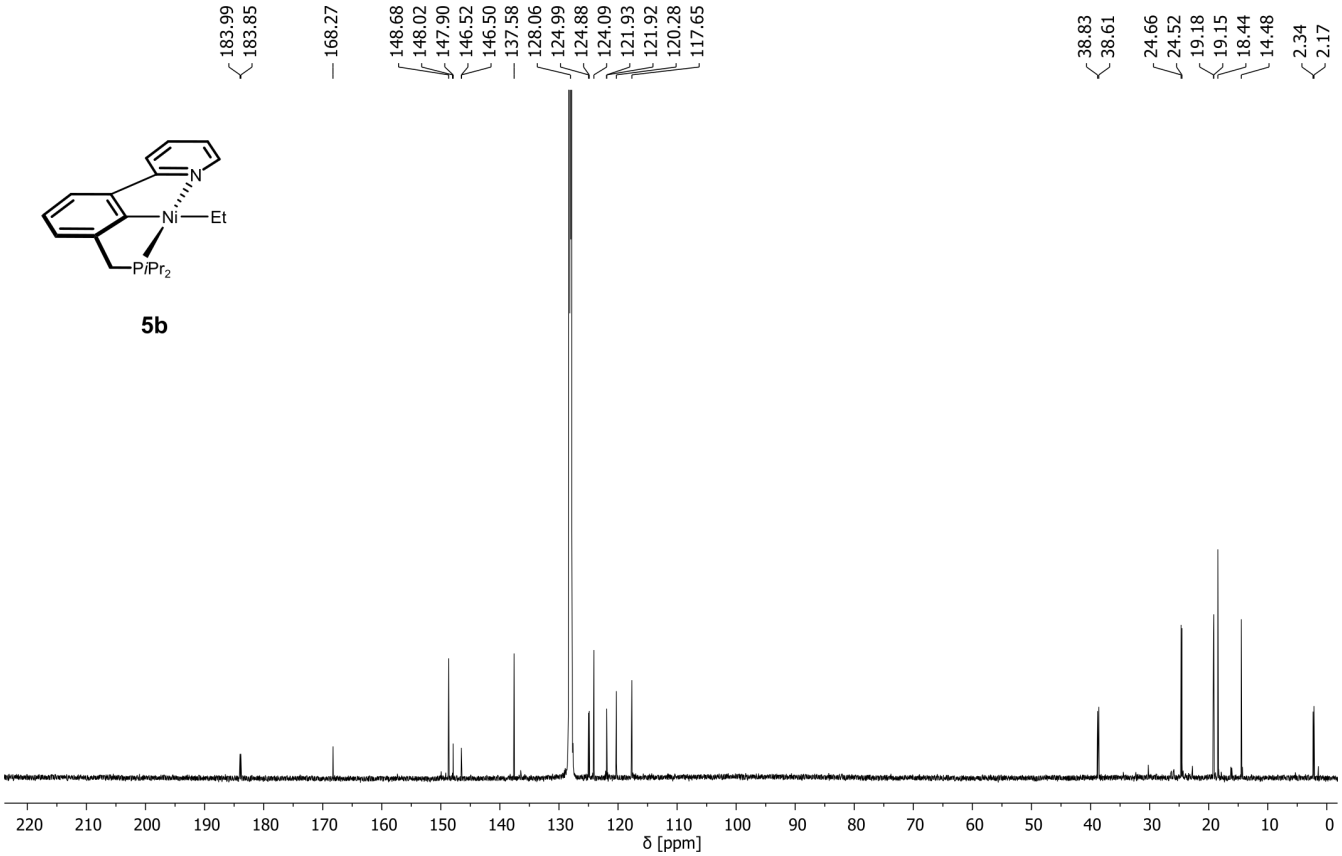

Figure S30. ^{13}C{^{1}H} (151 MHz, C_6D_6) [Ni($^{i\mathrm{Pr}}$PCN$^{\mathrm{CH_2}}$)(η^2-Et)]

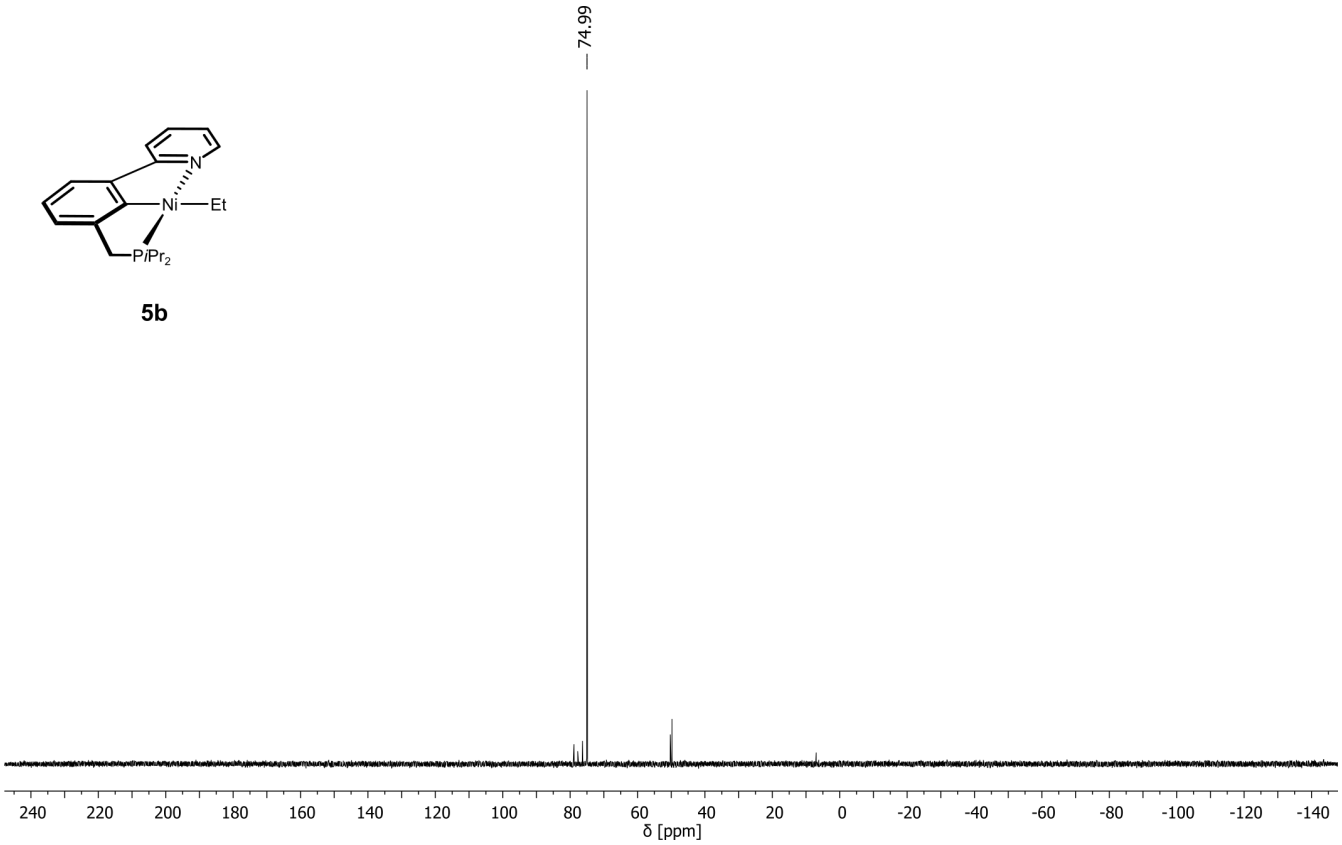

Figure S31. $^{31}P\{^{1}H\}$ (243 MHz, C_6D_6) [Ni(^{iPr}PCN^{CH_2})(η^2-Et)]

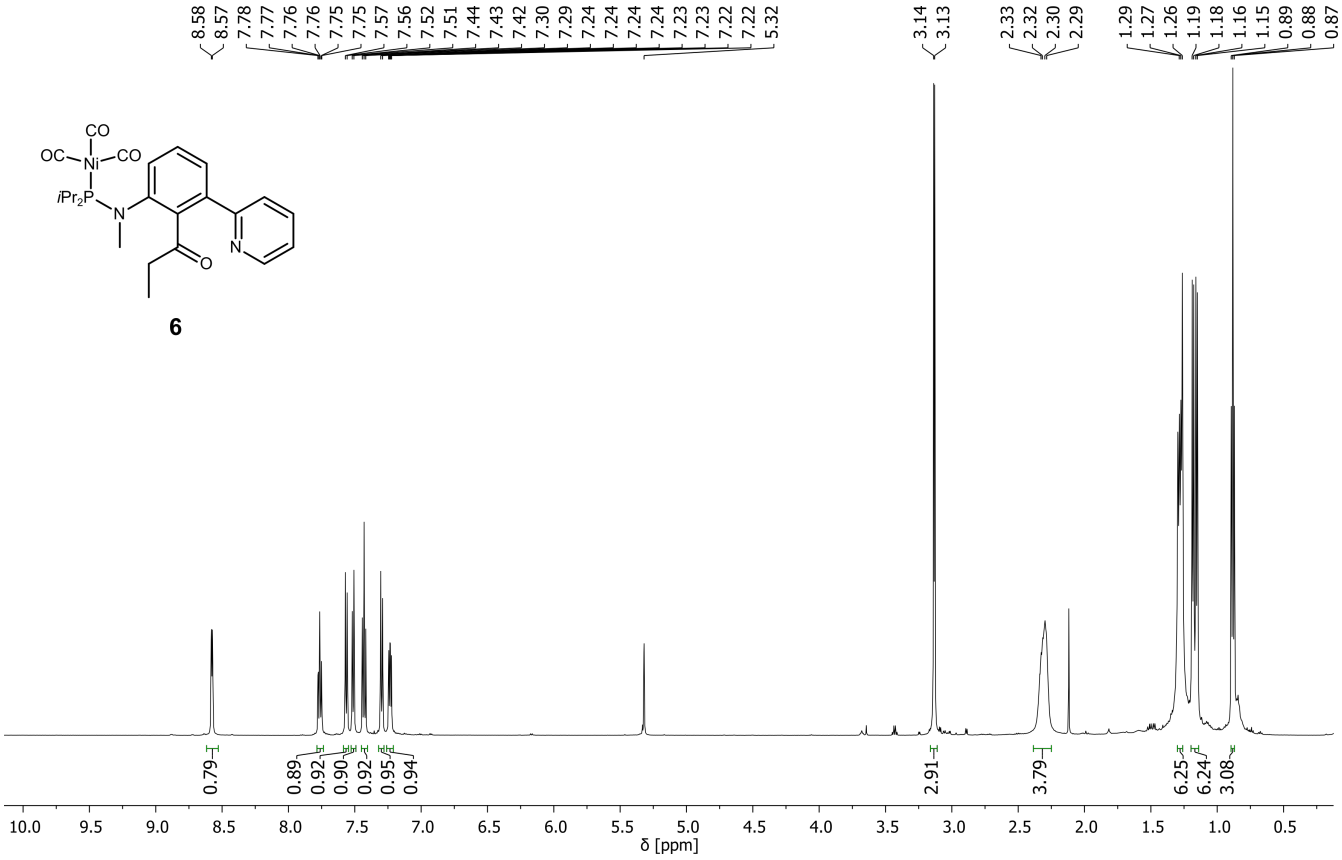

Figure S32. ^{1}H (600 MHz, CD_2Cl_2) [Ni($\kappa^1 P-{}^{iPr}$PC(COEt)N^{NMe})(CO)$_3$]

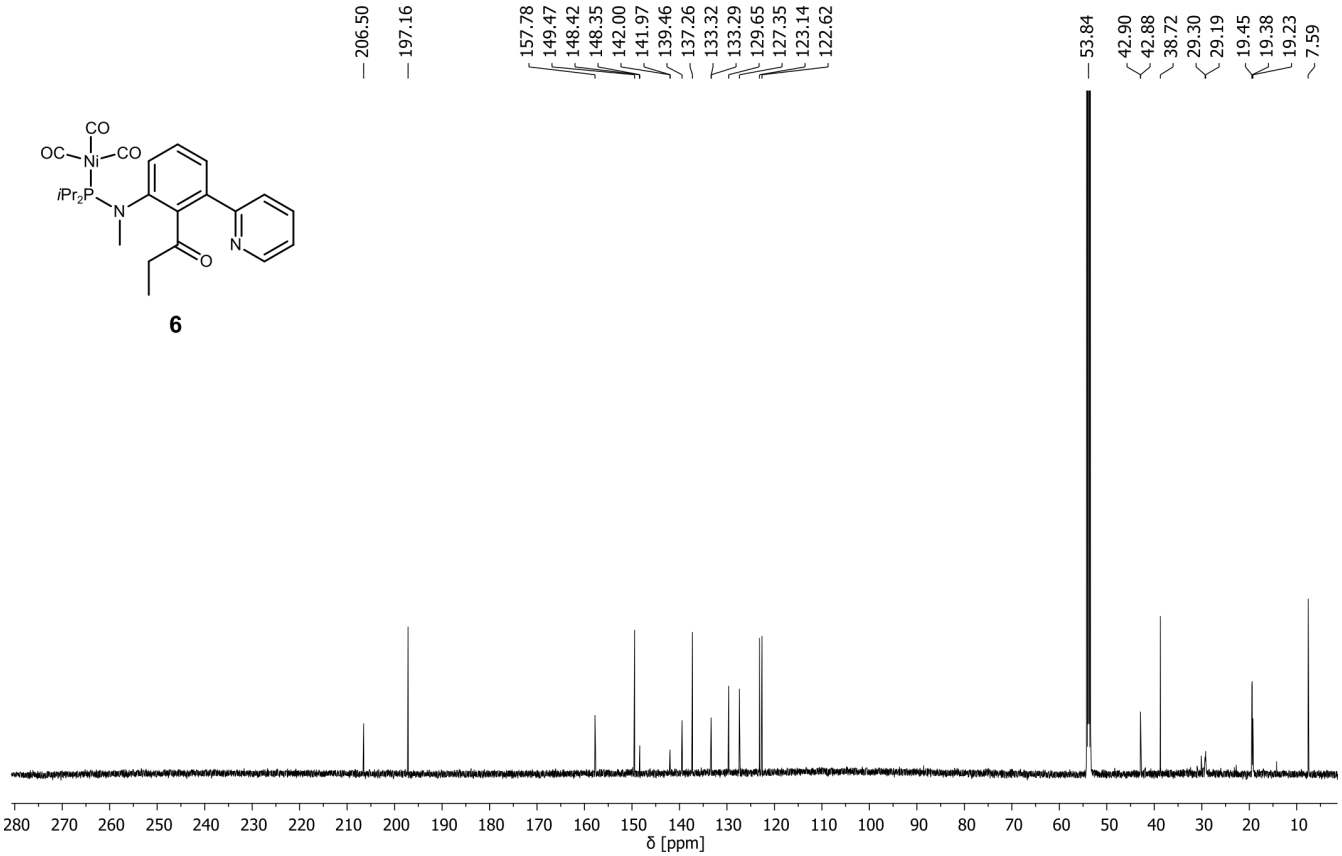

Figure S33. $^{13}C\{^{1}H\}$ (151 MHz, CD_2Cl_2) $[Ni(\kappa^1 P-{}^{iPr}PC(COEt)N^{NMe})(CO)_3]$

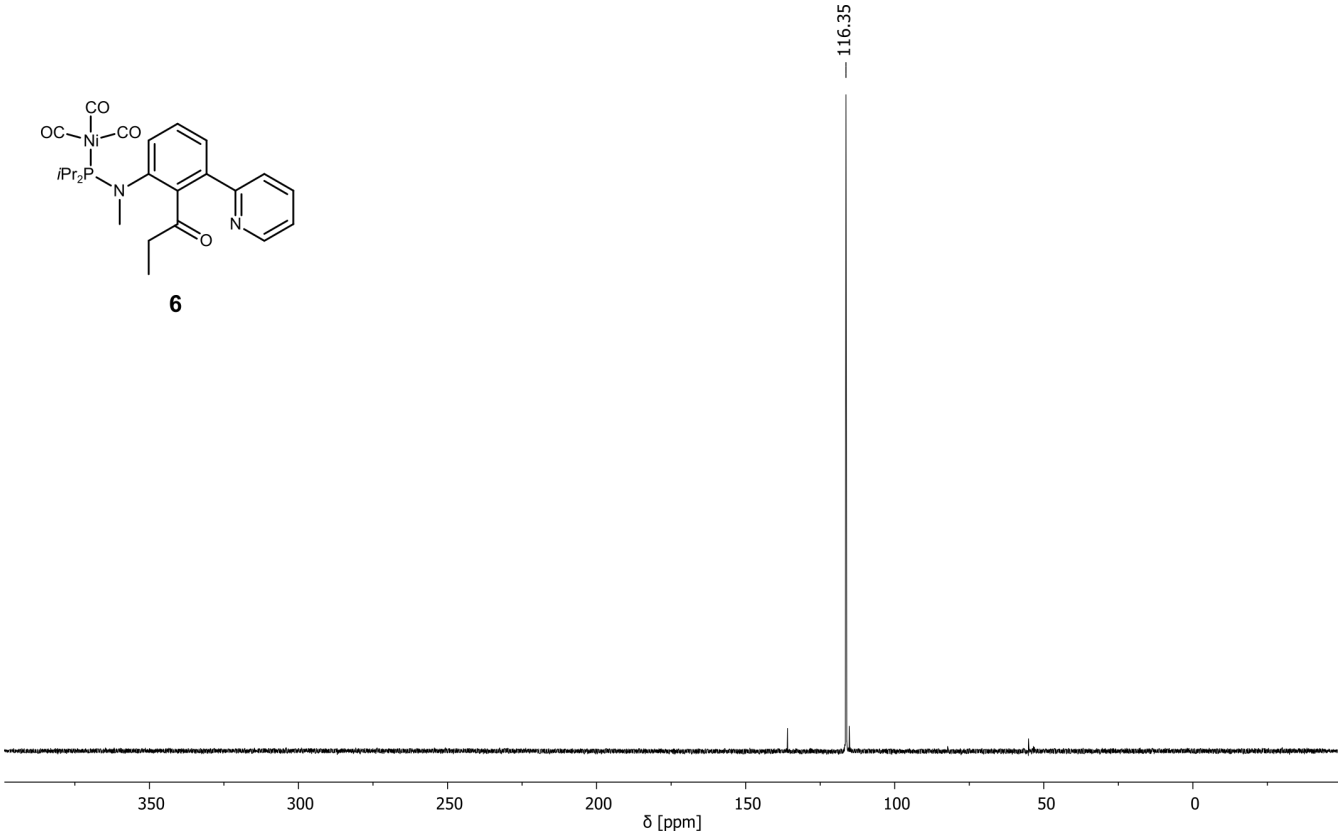

Figure S34. $^{31}P\{^{1}H\}$ (243 MHz, CD_2Cl_2) $[Ni(\kappa^1 P-{}^{iPr}PC(COEt)N^{NMe})(CO)_3]$

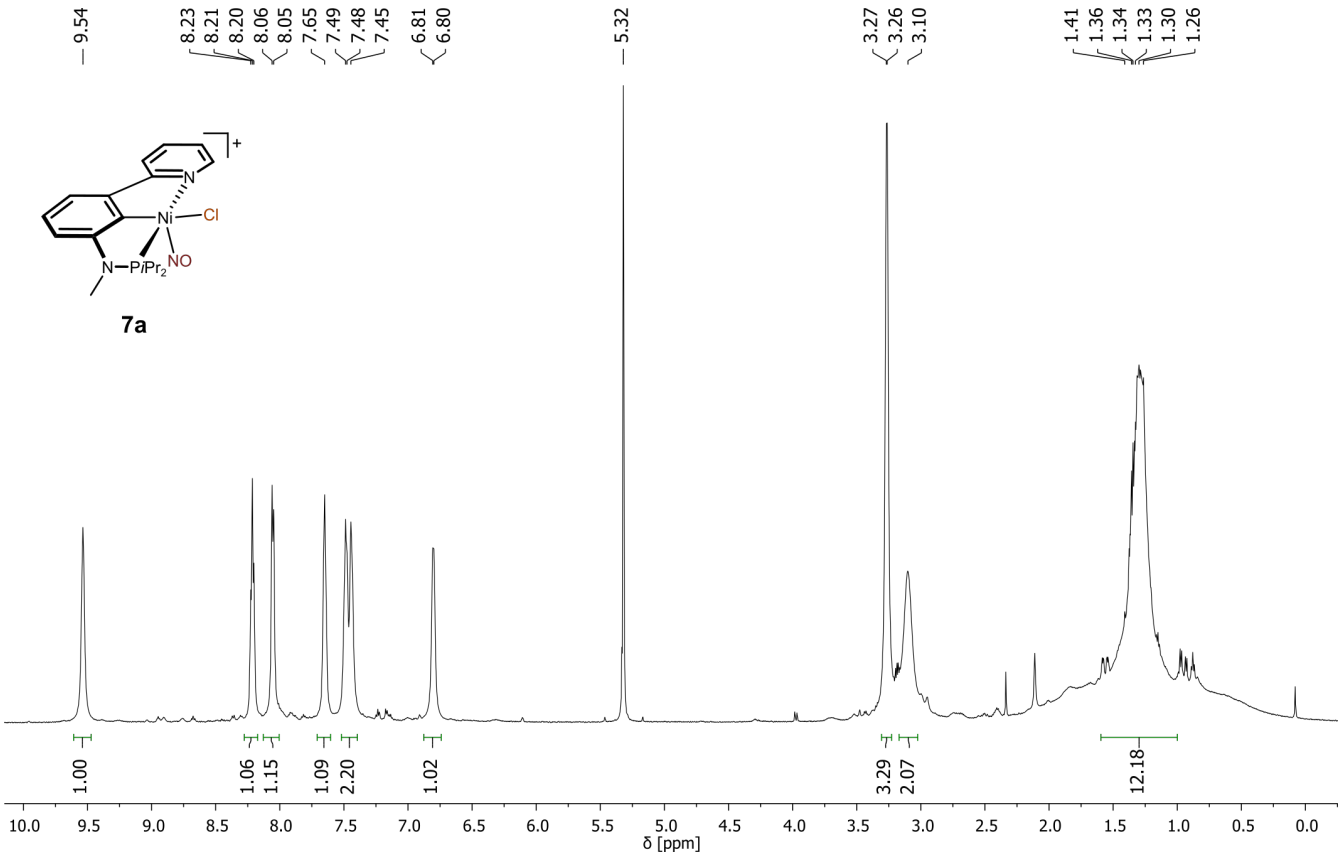

Figure S35. ^{1}H (600 MHz, CD_2Cl_2) [Ni($^{i\mathrm{Pr}}$PCN^{NMe})(NO)Cl]BF_4

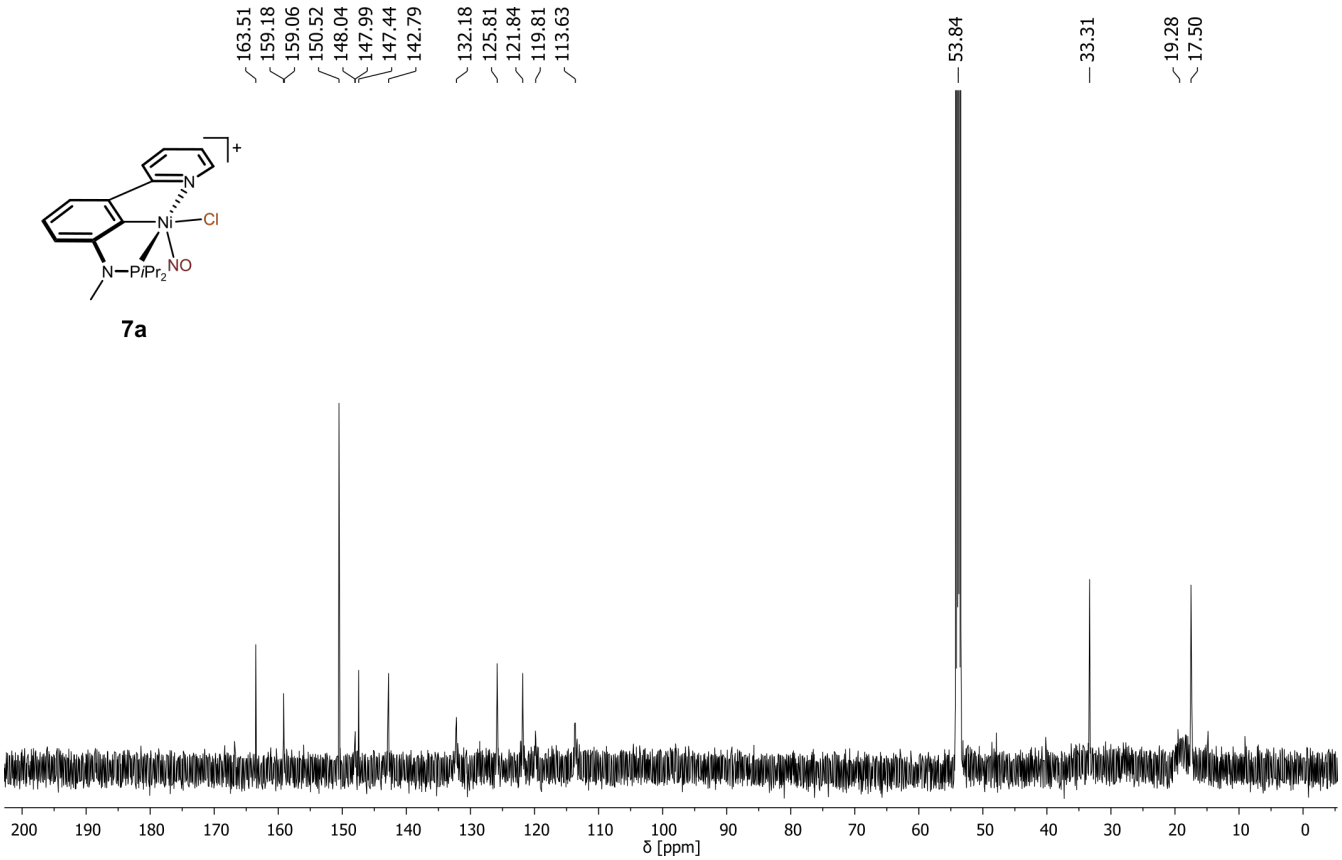

Figure S36. ^{13}C{^{1}H} (151 MHz, CD_2Cl_2) [Ni($^{i\mathrm{Pr}}$PCN^{NMe})(NO)Cl]BF_4

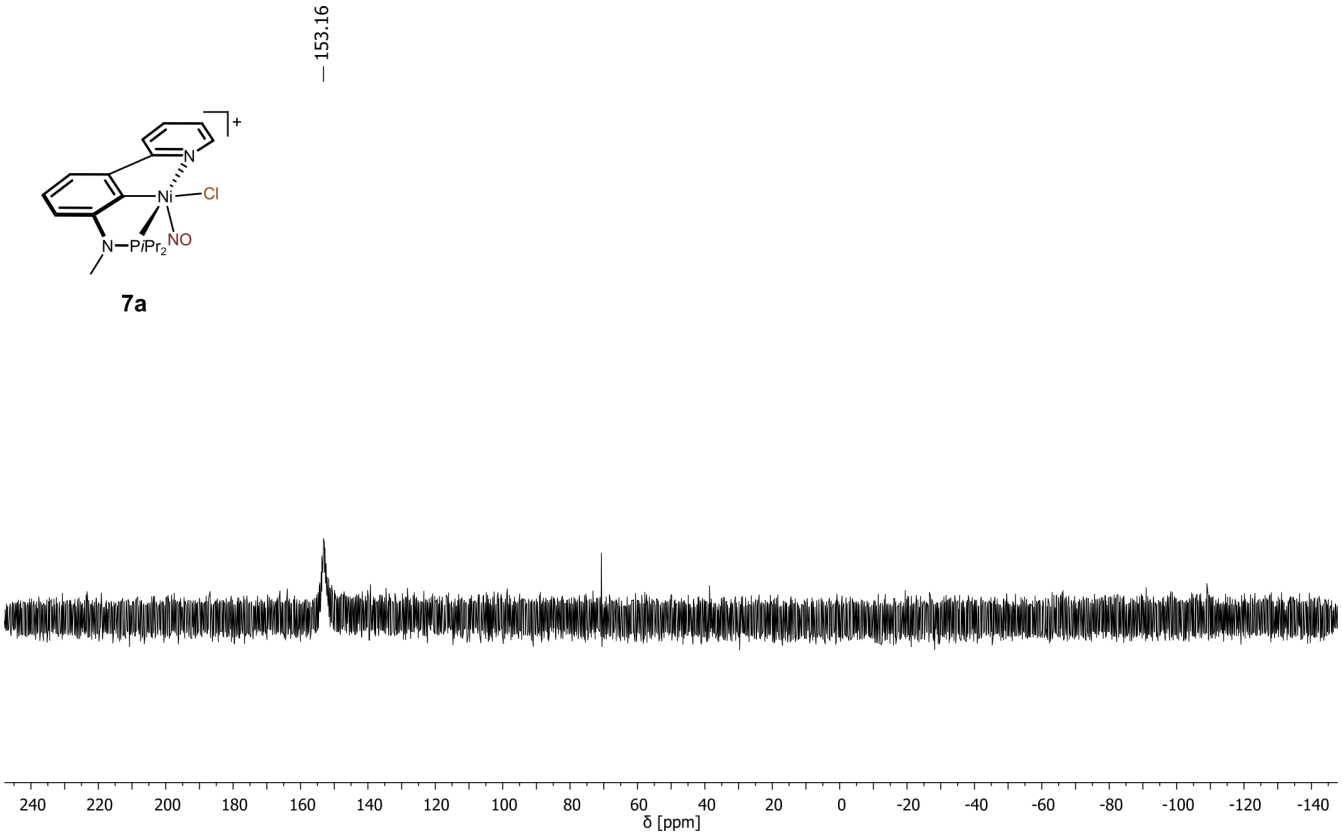

Figure S37. $^{31}P\{^{1}H\}$ (243 MHz, CD_2Cl_2) $[Ni(^{iPr}PCN^{NMe})(NO)Cl]BF_4$

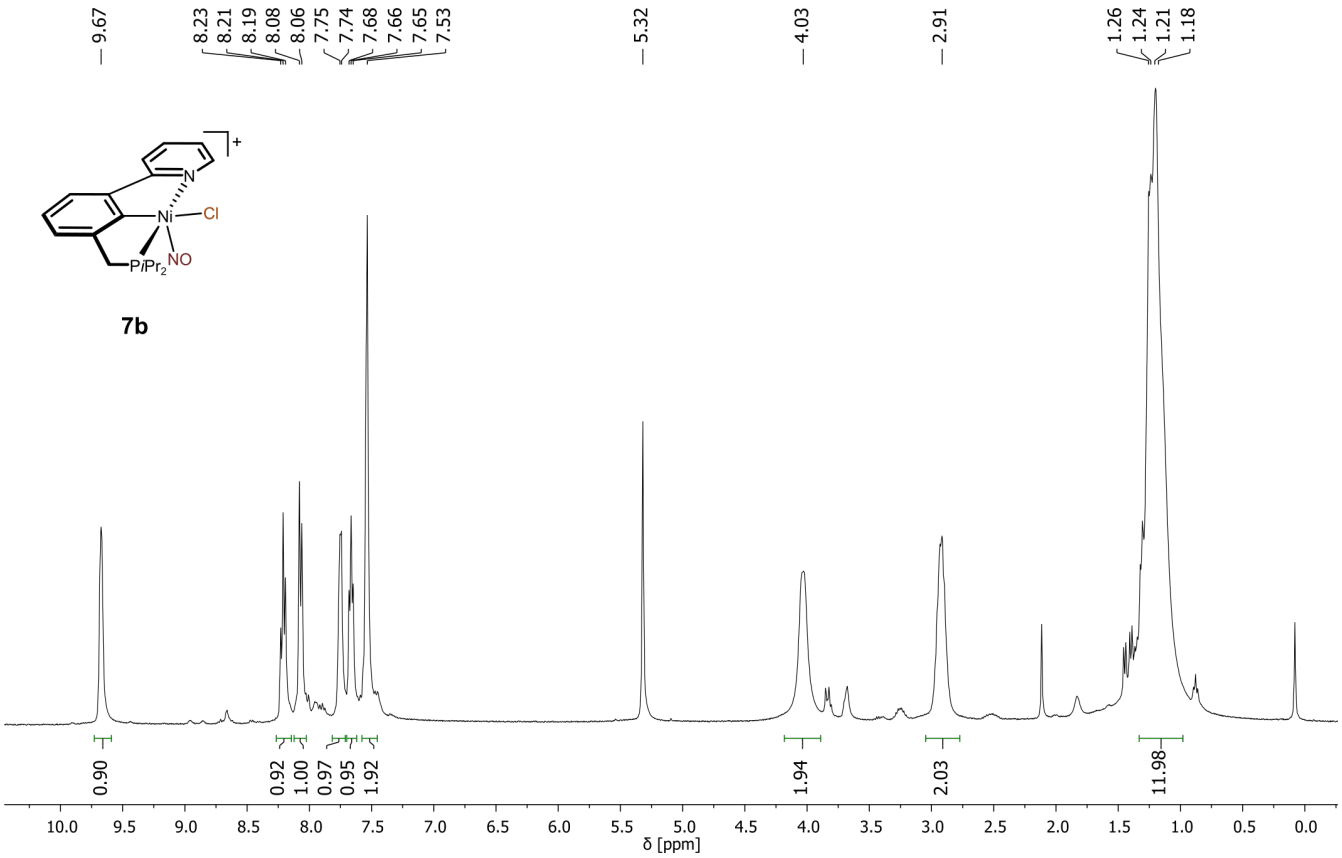

Figure S38. ^{1}H (400 MHz, CD_2Cl_2) $[Ni(^{iPr}PCN^{CH_2})(NO)Cl]BF_4$

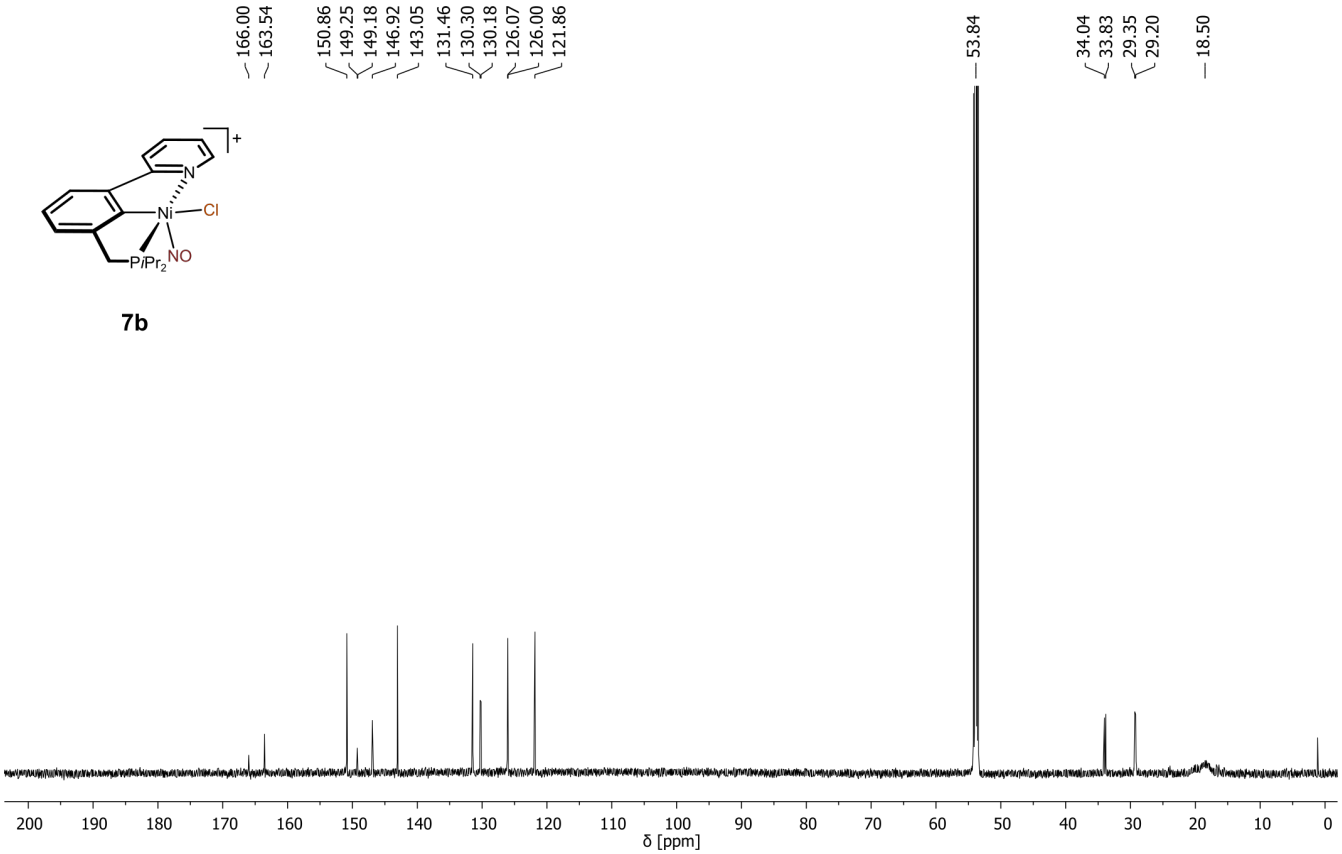

Figure S39. $^{13}C\{^{1}H\}$ (151 MHz, CD_2Cl_2) $[Ni(^{iPr}PCN^{CH_2})(NO)Cl]BF_4$

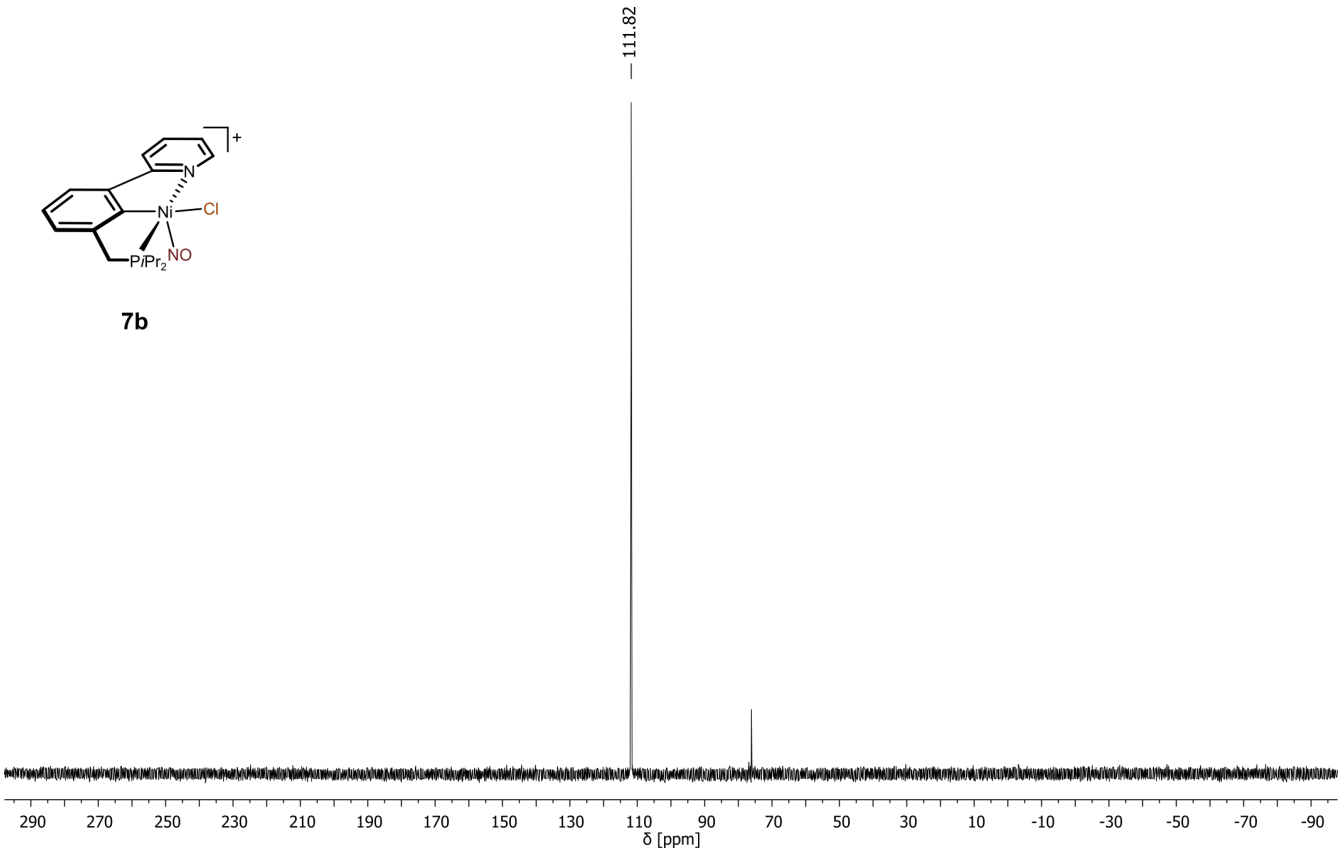

Figure S40. $^{31}P\{^{1}H\}$ (243 MHz, CD_2Cl_2) $[Ni(^{iPr}PCN^{CH_2})(NO)Cl]BF_4$

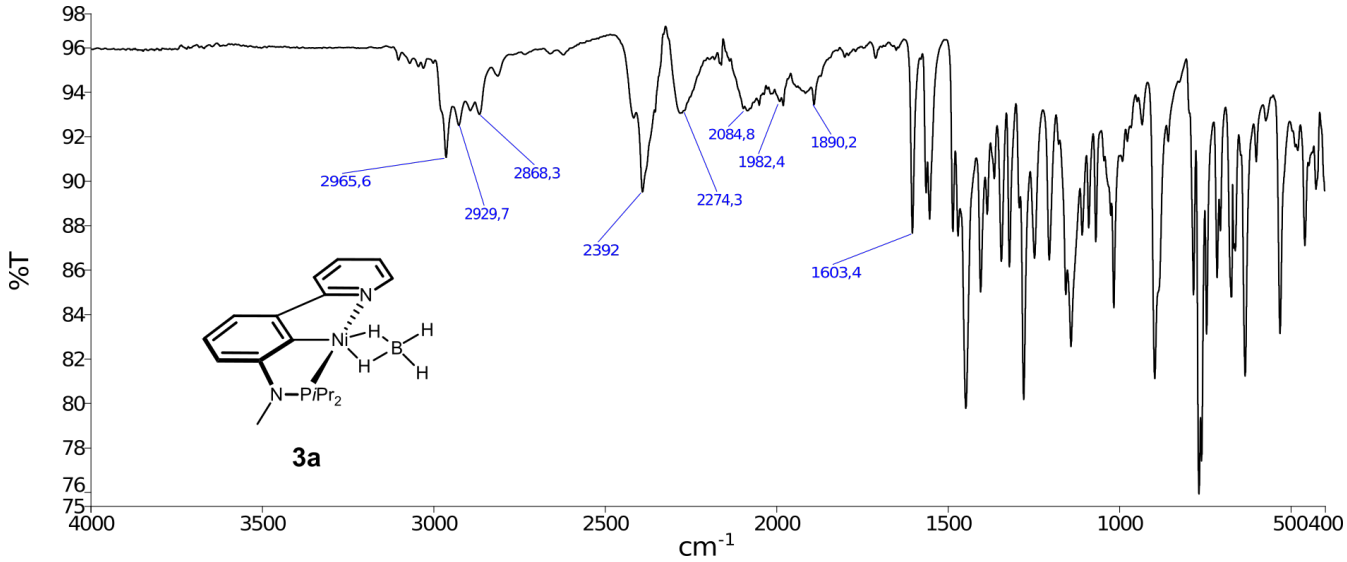

Figure S41. IR (ATR) [Ni(^{iPr}PCN^{NMe})(η^2-BH$_4$)]

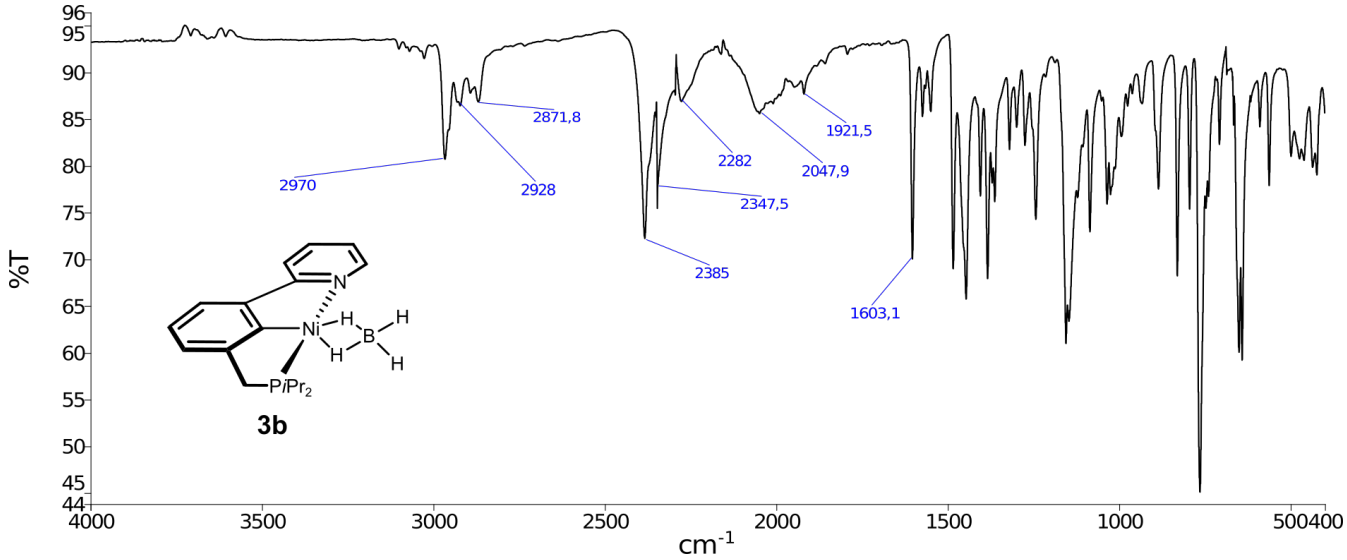

Figure S42. IR (ATR) [Ni(^{iPr}PCN^{CH_2})(η^2-BH$_4$)]

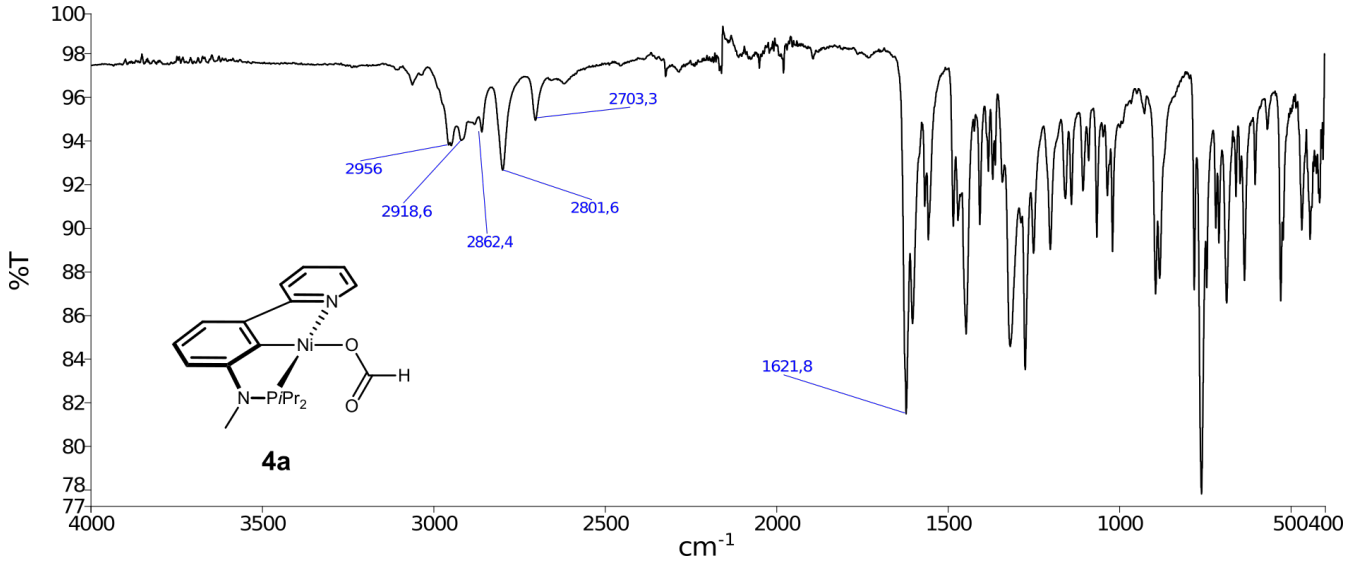

Figure S43. IR (ATR) [Ni(^{iPr}PCN^{NMe})(OCHO)]

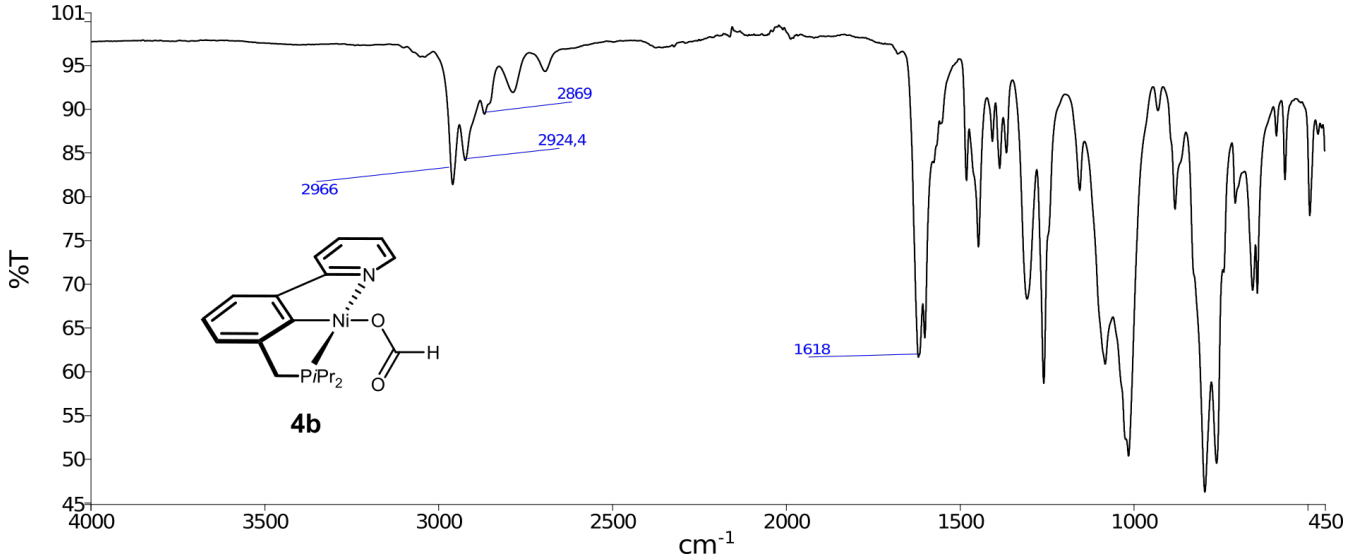

Figure S44. IR (ATR) [Ni(^{iPr}PCN^{CH_2})(OCHO)]

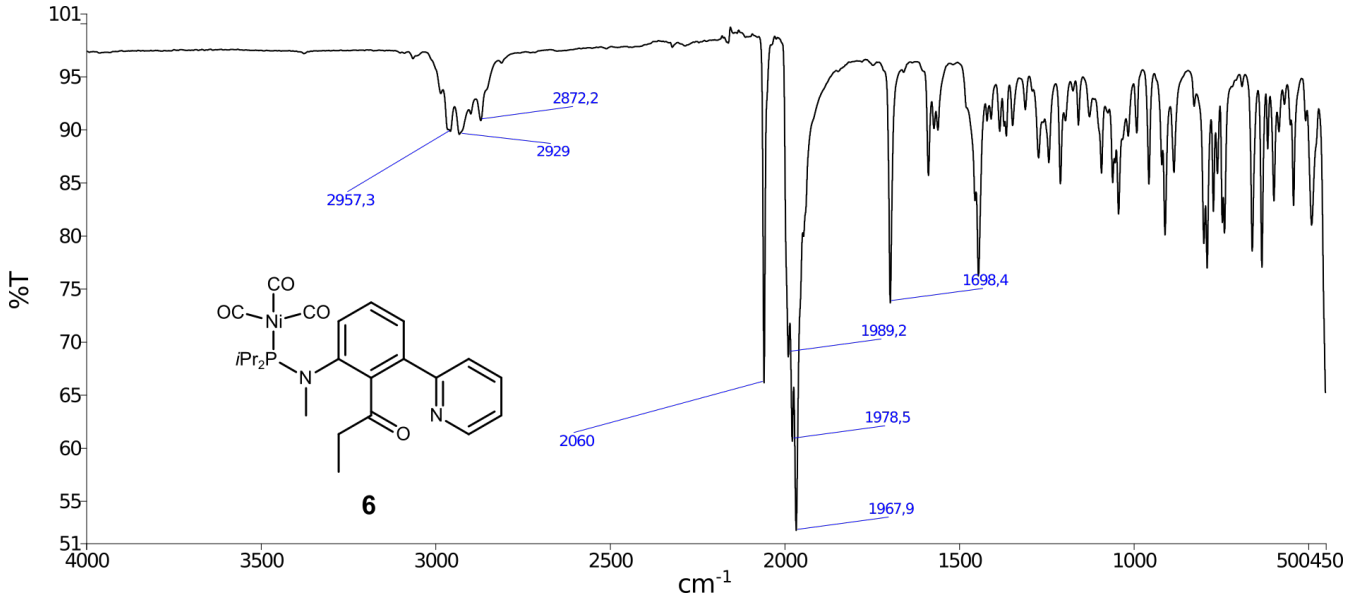

Figure S45. IR (ATR) [Ni($\kappa^1 P-^{i\mathrm{Pr}}$PC(COEt)N^{NMe})(CO)$_3$]

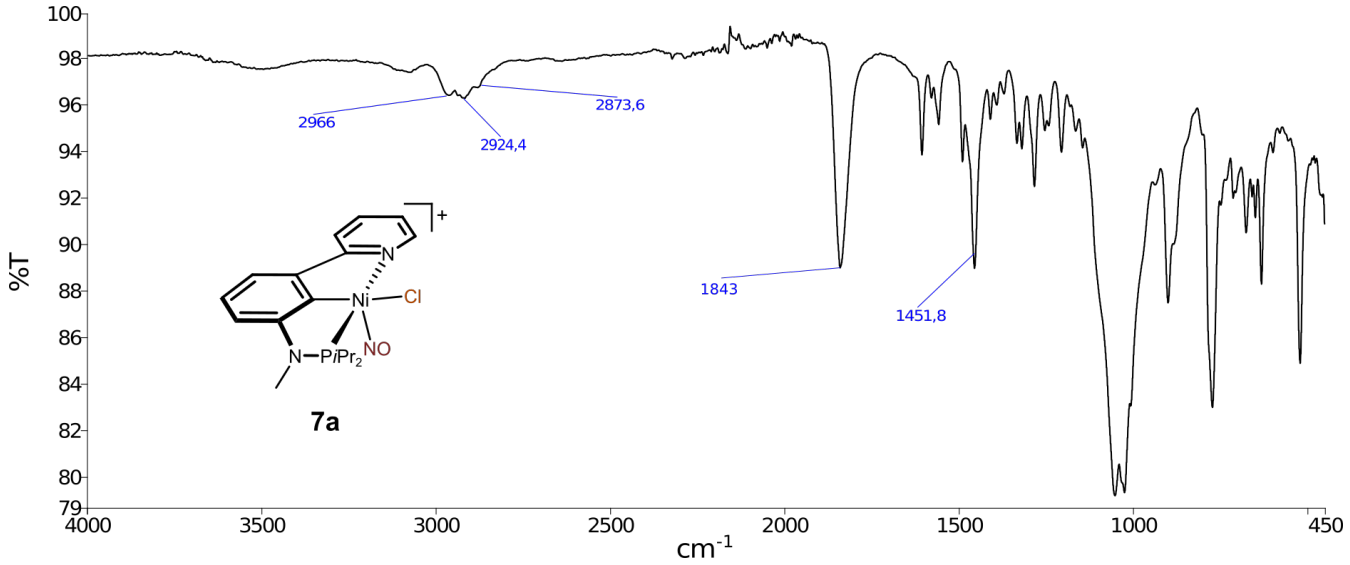

Figure S46. IR (ATR) [Ni($^{i\mathrm{Pr}}$PCN^{NMe})(NO)Cl]BF_4

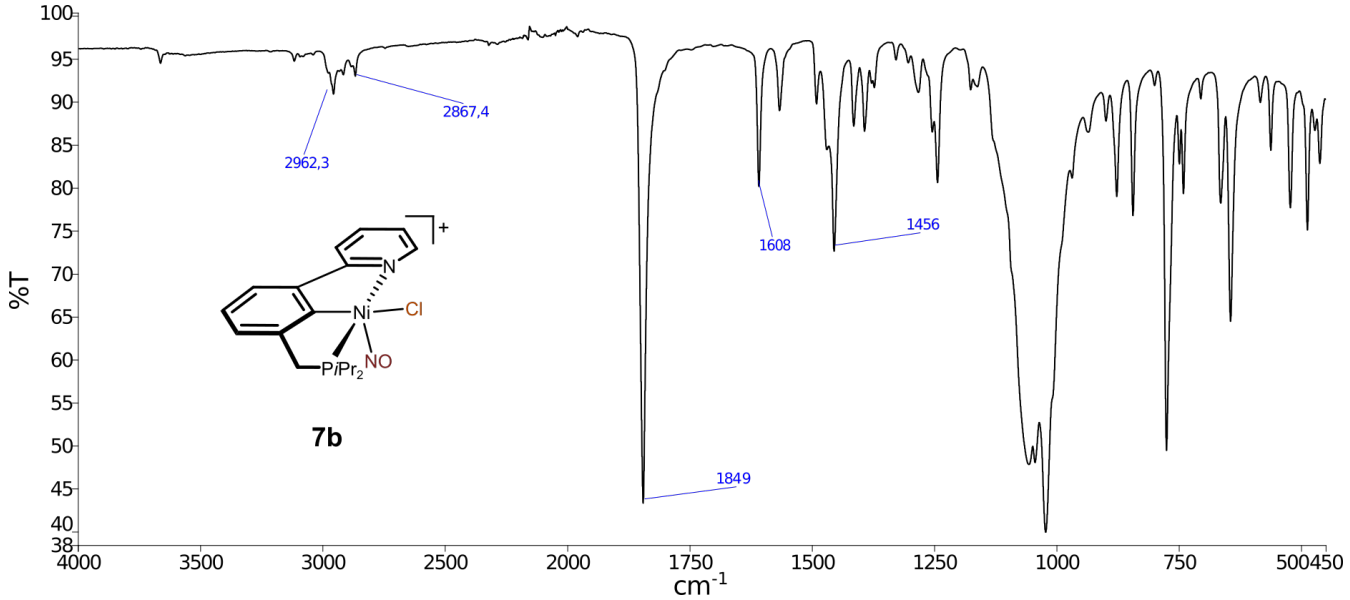

Figure S47. IR (ATR) [Ni($^{i\mathrm{Pr}}$PCN$^{\mathrm{CH_2}}$)(NO)Cl]BF_4

Table S1. Details for the crystal structure determinations of **2a** and **2b**.

complex	**2a**	**2b**
formula	$C_{18}H_{24}ClN_2NiP$	$C_{18}H_{23}ClNNiP$
cfw [g/mol]	393.52	378.50
cryst.size [mm]	0.33 × 0.26 × 0.15	0.30 × 0.16 × 0.04
color, shape	orange, rhombohedron	orange, plate
crystal system	orthorhombic	monoclinic
space group	P 2_1 2_1 2_1 (no. 19)	P 2_1 (no. 4)
a [Å]	11.5919(13)	7.0029(5)
b [Å]	11.6869(13)	11.1655(8)
c [Å]	40.865(5)	11.3875(8)
α [deg]	90	90
β [deg]	90	95.976(2)
γ [deg]	90	90
V [$Å^3$]	5536.1(11)	885.56(11)
T [K]	100	100
Z	12	2
$\rho_{calc.}$ [g cm^{-3}]	1.416	1.419
μ [mm^-1] (MoKα)	1.283	1.332
F (000)	2472	396
absorption corrections	multi-scan	multi-scan
T_{min}-T_{max}	0.64-0.75	0.54-0.75
Θ range [deg]	1.83-30.50	2.93-32.59
no. of rflns measd	80394	14081
R_{int}	0.0498	0.0385
no. of rflns unique	16857	6426
no. of rflns $I > 2\sigma(I)$	14879	5714
no. of params/restraints	638/0	203/1
R ($I > 2\sigma(I)$) [(a)]	0.0360	0.0332
R (all data)	0.0447	0.0402
wR ($I > 2\sigma(I)$)	0.0752	0.0630
wR (all data)	0.0781	0.0653
GooF	1.038	0.976
Diff. Four. peaks min/max [$eÅ^{-3}$]	-0.37 / 0.85	-0.33 / 0.68

[(a)] $R = \sum ||F_0| - |F_c|| / \sum |F_0|$, $wR = \sum w(|F_0| - |F_c|) / \sum w|F_0|$, $GooF = \{\sum[w(F_0^2 - F_c^2)^2]/(n-p)\}^{(1/2)}$

Table S2. Details for the crystal structure determinations of **3a**, **3b** and **4a**.

complex	**3a**	**3b**	**4a**
formula	$C_{18}H_{28}BN_2NiP$	$C_{18}H_{27}BNNiP$	$C_{19}H_{25}N_2NiO_2P$
cfw [g/mol]	372.91	357.89	403.09
cryst.size [mm]	0.60 × 0.30 × 0.10	0.27 × 0.25 × 0.18	0.34 × 0.14 × 0.10
color, shape	orange, plate	red, block	orange rod
crystal system	orthorhombic	orthorhombic	monoclinic
space group	P 2_1 2_1 2_1 (no. 19)	P 2_1 2_1 2_1 (no. 19)	P 2_1/n (no. 14)
a [Å]	11.6053(6)	11.0453(5)	8.5996(14)
b [Å]	11.7634(5)	12.6018(6)	11.0978(19)
c [Å]	41.3413(19)	13.2352(6)	20.150(3)
α [deg]	90	90	90
β [deg]	90	90	101.983(4)
γ [deg]	90	90	90
V [$Å^3$]	5643.8(5)	1842.22(15)	1881.2(5)
T [K]	100	100	100
Z	12	4	4
$\rho_{calc.}$ [g cm^{-3}]	1.317	1.290	1.423
μ [mm^-1] (MoKα)	1.116	1.136	1.131
F (000)	2376	760	848
absorption corrections	multi-scan	multi-scan	multi-scan
T_{min}-T_{max}	0.59-0.75	0.27-0.35	0.21-0.27
Θ range [deg]	1.80-36.79	2.45-39.97	3.04-32.87
no. of rflns measd	146486	26315	24206
R_{int}	0.0593	0.0347	0.0454
no. of rflns unique	28191	10914	6946
no. of rflns $I > 2\sigma(I)$	23500	8841	5292
no. of params/restraints	685/0	219/0	231/0
R ($I > 2\sigma(I)$) [(a)]	0.0398	0.0326	0.0359
R (all data)	0.0559	0.0465	0.0552
wR ($I > 2\sigma(I)$)	0.0741	0.0654	0.0855
wR (all data)	0.0793	0.0697	0.0938
GooF	1.009	0.954	1.024
Diff. Four. peaks min/max [e$Å^{-3}$]	-0.56 / 0.76	-0.37 / 0.56	-0.29 / 0.82

[(a)] $R = \sum ||F_0| - |F_c|| / \sum |F_0|$, $wR = \sum w(|F_0| - |F_c|) / \sum w|F_0|$, $GooF = \{\sum[w(F_0^2 - F_c^2)^2]/(n-p)\}^{(1/2)}$

Table S3. Details for the crystal structure determinations of **5a** and **5b** (measured at 100 and 270 K).

complex	**5a**	**5b**	**5b**
formula	$C_{20}H_{29}N_2NiP$	$C_{20}H_{28}NNiP$	$C_{20}H_{28}NNiP$
cfw [g/mol]	387.13	372.11	372.11
cryst.size [mm]	0.42 × 0.40 × 0.08	0.24 ×0.08 × 0.06	0.24 × 0.08 × 0.06
color, shape	red, plate	red, rod	red, rod
crystal system	orthorhombic	triclinic	trigonal
space group	P c a 2_1 (no. 29)	P $\overline{1}$ (no. 2)	P $\overline{3}$ (no. 148)
a [Å]	12.3137(4)	8.9137(11)	33.3732(11)
b [Å]	14.8397(4)	19.328(2)	33.3732(11)
c [Å]	10.5568(3)	19.358(2)	9.0041(3)
α [deg]	90	117.679(3)	90
β [deg]	90	98.732(4)	90
γ [deg]	90	98.233(3)	120
V [Å^3]	1929.06(10)	2830.8(6)	8684.9(6)
T [K]	100	100	270
Z	4	6	18
$\rho_{calc.}$ [g cm^{-3}]	1.333	1.310	1.281
μ [mm$^-$1] (MoKα)	1.092	1.112	1.087
F (000)	824	1188	3564
absorption corrections	multi-scan	multi-scan	multi-scan
T_{min}-T_{max}	0.60-0.75	0.28-0.34	0.28-0.34
Θ range [deg]	2.75-35.31	2.38-30.43	2.37-30.12
no. of rflns measd	20902	61181	67968
R_{int}	0.0338	0.0583	0.0493
no. of rflns unique	8423	16912	5693
no. of rflns $I > 2\sigma(I)$	7393	12955	4004
no. of params / restraints	223/1	667/0	218/0
R ($I > 2\sigma(I)$) $^{(a)}$	0.0309	0.0625	0.0400
R (all data)	0.0383	0.0918	0.0685
wR ($I > 2\sigma(I)$)	0.0753	0.1353	0.0907
wR (all data)	0.0786	0.1517	0.1028
GooF	1.049	1.052	1.037
Diff. Four. peaks min/max [eÅ^{-3}]	-0.422 / 0.931	-0.972 / 0.098	-0.213 / 0.428

$^{(a)} R = \sum ||F_0| - |F_c|| / \sum |F_0|$, $wR = \sum w(|F_0| - |F_c|) / \sum w|F_0|$, $GooF = \{\sum[w(F_0^2 - F_c^2)^2]/(n-p)\}^{(1/2)}$

Table S4. Details for the crystal structure determinations of **6** and **7b**.

complex	**6**	**7b**
formula	$C_{24}H_{29}N_2NiO_4P$	$C_{18.50}H_{24}BCl_2F_4N_2NiOP$
cfw [g/mol]	499.17	537.79
cryst.size [mm]	0.47 × 0.15 × 0.04	0.30 × 0.24 × 0.03
color, shape	yellow, rod	green, plate
crystal system	monoclinic	monoclinic
space group	P 2_1/c (no. 14)	P 2_1/c (no. 14)
a [Å]	17.4084(16)	25.806(3)
b [Å]	9.4781(9)	11.6896(14)
c [Å]	14.7189(15)	15.1119(19)
α [deg]	90	90
β [deg]	92.451(2)	93.334(4)
γ [deg]	90	90
V [Å^3]	2426.4(4)	4551.0(10)
T [K]	100	100
Z	4	8
$\rho_{calc.}$ [g cm^{-3}]	1.366	1.570
μ [mm^{-}1] (MoKα)	0.897	1.204
F (000)	1048	2200
absorption corrections	multi-scan	multi-scan
T_{min}-T_{max}	0.40-0.49	0.65-0.75
Θ range [deg]	2.34-30.04	0.79-28.47
no. of rflns measd	7097	118300
R_{int}	-	0.1175
no. of rflns unique	7097	11470
no. of rflns $I > 2\sigma(I)$	5598	7508
no. of params / restraints	296/0	580/0
R ($I > 2\sigma(I)$) $^{(a)}$	0.0461	0.0425
R (all data)	0.0727	0.0902
wR ($I > 2\sigma(I)$)	0.0909	0.0892
wR (all data)	0.1007	0.1101
GooF	1.008	0.901
Diff. Four. peaks min/max [eÅ^{-3}]	-0.38 / 0.46	-0.67 / 0.70

$^{(a)} R = \sum ||F_0| - |F_c|| / \sum |F_0|$, $wR = \sum w(|F_0| - |F_c|) / \sum w|F_0|$, $GooF = \{\sum[w(F_0^2 - F_c^2)^2]/(n-p)\}^{(1/2)}$

References

(1) Padmanabhan, S.; Reddy, N. L.; Durant, G. J. A convenient one pot procedure for N-methylation of aromatic amines using trimethyl orthoformate. *Synthetic communications*

1997, *27*, 691–699.

(2) Muntaner, J. G.; Casarrubios, L.; Sierra, M. A. Synthesis of new bioorganometallic Ir-and Rh-complexes having β-lactam containing ligands. *Organic & Biomolecular Chemistry* **2014**, *12*, 286–297.

(3) Wang, Y.; Qin, C.; Jia, X.; Leng, X.; Huang, Z. An Agostic Iridium Pincer Complex as a Highly Efficient and Selective Catalyst for Monoisomerization of 1-Alkenes to trans-2-Alkenes. *Angewandte Chemie International Edition* **2017**, *56*, 1614–1618.